

# 1 FINAL PUBLISHABLE SUMMARY

1.1 EXECUTIVE Summary .....	1
1.2 Project context and objectives .....	2
1.3 Description of the main results .....	4
1.3.1 Narrow Gap Dissimilar Metal Weld Integrity - Large scale test on Mock-up 1 (MU1)..	4
1.3.2 Effects of residual stress and thermal ageing on ductile fracture - Large scale test on Mock-up 2 .....	9
1.3.3 Transferability in Clad pipes - Large scale test on Mock-up 3 (MU3) .....	12
1.3.4 Weld residual stress simulation and measurement (MU4 results) .....	16
1.3.5 Stress Corrosion Cracking .....	20
1.3.6 Thermal fatigue through turbulent mixing.....	23
1.3.7 Dynamic and impact effects - Mock-up 7.....	27
1.3.8 LBB approaches and Engineering Assessment Methods.....	30
1.3.9 Training.....	34
1.3.10 Main project conclusions (final summary) .....	34
1.4 Potential impact, exploitation of results and main dissemination activities.....	38
1.5 Style Consortium, Web Site and contact details .....	40

## 1.1 EXECUTIVE SUMMARY

The overall objective of the STYLE project has been to assess, optimise and develop the use of advanced tools for the structural integrity assessment of reactor coolant pressure boundary components relevant to ageing and life time management. The range of assessment tools considered has included those for assessment of component failure by advanced fracture mechanics analyses, validated on small and large scale experiments, quantification of weld residual stresses by numerical analysis and by measurements, stress corrosion crack initiation/growth effects, and assessment of RCPB components under dynamic and seismic loading.

Several technical issues have been addressed in STYLE. These include:

- Dissimilar metal weld integrity,
- Effect of weld residual stress on fracture and damage modelling,
- Weld residual stress simulation and measurement with and without weld repairs,
- Transferability of material properties,
- Stress corrosion cracking,
- Thermal fatigue through turbulent mixing,
- Dynamic impact testing and FE analysis,
- Benchmarking of engineering assessment methods and leak-before-break approaches.

The STYLE project has been largely centred on structural mock-ups and supporting experiments from small to large scale. The overall aim of the project was to establish enhanced tools and methodologies to be applied in lifetime assessments of pipes and associated components. Highly sophisticated experimental and computational methods and advanced tools have been developed, in order to realistically describe the complex physical mechanisms leading to ageing and failure of the reactor coolant system piping and components. Various European Leak-before-break (LBB) and

engineering assessment (EAM) methods to predict the integrity of welds and weld repair issues, including manufacturing procedures, qualification of inspection techniques and mitigation measures have been compared within the project and validated against the mock-up experiments.

The STYLE project has made significant achievements, but there is still further work required in order to enhance the structural integrity understanding and best practice guidance for nuclear piping systems and associated components. This work includes:

- Properly quantifying and understanding the levels of conservatism in current integrity assessment methods with a view to revising guidance and procedures using data which have been produced during the STYLE project
- Consolidating results in the form of best practice guidelines for harmonization of procedures for fracture toughness assessment (testing and integrity) of dissimilar metal welds
- Further developing advanced tools for structural integrity assessment and plant lifetime management
- Benchmarking safety assessment methodologies including comparison of outputs from deterministic versus probabilistic methods and integration into the safety assessment
- Completing the knowledge of material properties and their testing techniques for relevant materials.

## **1.2 PROJECT CONTEXT AND OBJECTIVES**

The safety and reliability of all systems has to be maintained throughout the lifetime of a nuclear power plant. Continuous R&D work is needed in targeted areas to meet the challenges of long term operation of existing designs and for the GEN-III designs. A special focus is placed on reactor coolant pressure boundary, because its integrity and functionality from the time of first operation until end of life is required to ensure plant safety.

The overall objective of STYLE has been to assess, optimize and develop the use of advanced tools for the structural integrity assessment of RCPB components relevant to ageing and life time management and to support the integration of the knowledge created in the project into mainstream nuclear industry assessment codes.

The project concept has been based on carefully selected research topics, which thematically cover the complex multidisciplinary character of structural assessment of RCPB components. The prioritisation of the work reflects the needs of industrial end-users and assessment of currently available techniques and data at European and international level. The "STYLE TOOLS" End Product consolidates the results in the form of best practice guidelines on structural assessment and life time management of the RCPB in European nuclear power plants.

STYLE has comprised of 7 main work packages, which have following objectives:

### **WP1 Experimental Work**

The main objectives of the WP1 have been to perform manufacturing and material characterization for all planned mock-ups, which have been dedicated for the further development and validation of numerical and analytical assessment tools. Under the most challenging tasks within WP1 has been the preparation and execution of three large scale fracture tests:

-The first Mock-up provided by AREVA was a pipe with a narrow gap dissimilar weld (DMW). The pipe thickness was approximately 40 mm and the outer diameter 352 mm. This first Mock-up was in effect, a continuation of the ADIMEW project and dealt with the improvement of the assessment for DMW and Leak-before-break procedures.

- The second Mock-up, provided by EDF Energy (former British Energy), was an austenitic steel butt-welded pipe with a weld repair austenitic weld (Outer diameter: 180 mm – thickness: 35 mm). This mock-up was aimed at the development and validation of defect assessment techniques for austenitic steels in the presence of weld residual stresses. Other complex factors, such as the consideration of crack tip constraint also came into consideration.

- The third Mock-up was a clad ferritic pipe provided by AREVA GmbH (Outer diameter: 424 mm – thickness: 31 mm + 5 mm stainless steel cladding), which focused mainly on transferability problems in the assessment procedure and the treatment of cladding.

Mock-up 4 was dedicated to develop more realistic residual stress profiles. Such profiles are used to assess the integrity of pipe girth welds. The effect of the heat input (10 and 25 kJ/cm) on the resulting residual stress profile was investigated. RS measurements such as iDHD measurements were performed and compared with each other and with results of numerical weld simulations.

Mock-up 6 was a 1:5 scale modified replica of the VVER-440 primary feed water nozzle safe end dissimilar metal weld, which was dedicated for validation of the weld simulation approach developed in a combination with the performed residual stress measurements (Barkhausen noise, DHD and neutron diffraction).

Mock-up 7 was designed to evaluate the influence of dynamic effects (wave propagation and inertia effects) on crack tip loading in a pipe. The material used was 16Mo3 high quality ferritic construction steel. The wall thickness of the pipe  $t = 8.5$  mm and the outer diameter  $D = 114$  mm.

A part of the STYLE program under WP1 was the material characterization under environmental conditions. The work was focused on crack initiation and crack growth rate tests of an industrially produced narrow gap IN52 weld on a steel block. The different corrosion tests were aimed to reveal whether this material is susceptible to stress corrosion cracking or not. Corrosion tests were carried out under simulated PWR primary water conditions.

## **WP2 Numerical Analyses/Advanced Tools**

The main goal of WP2 was to develop highly sophisticated methods and advanced tools, which are able to describe realistically the complex physical mechanisms leading to ageing and failure of the reactor coolant system piping and components. A further important objective was to perform design of mock-ups and specimens as well as the interpretation of tests conducted within WP1.

## **WP3 Engineering Assessment Methods (EAM), Leak-Before-Break (LBB) Analyses**

The general aim of the WP was to firstly establish the state of the art national practices (including evolution, particularly in terms of LBB) and approaches in LBB and EAM, both from a deterministic and a probabilistic point of view. The approaches (i.e. procedures and codes where applicable) were then applied/validated against Mock-up experiments and analytical case studies. The information obtained from these was intended to enable best practice guidance to be recommended on the various elements of LBB and EAM

#### **WP4 Knowledge and Data Management**

The main goal of WP4 was to establish a comprehensive assessment of the available technology related to the Leak Before Break concept and other assessment methods as well as to collect information on selected aspects related to welding and weld repair in primary piping components of nuclear power Plants. Further task of WP 4 was to develop and maintain the project web site.

#### **WP5 Training activities**

The main goal of WP5 was to facilitate the training of eligible new scientists and engineers. Training has been provided in the development of project end product via short visits to the relevant partner establishments. In addition to the training visits dedicated workshops have also been held during the project.

#### **WP6 End User Group**

The objectives of the WP6 was to establish a firm “need for information” basis in the form of an issue matrix in the area to validate the project, to review the outcome of the respective work packages and to establish a platform under which the results could be implemented and put to use for the end user participants and other relevant partners of the STYLE project.

#### **WP7 End Product**

WP7 was intended to integrate the work undertaken in WP’s 1 to 5 in a form suitable for wider dissemination and adoption. This end product is called "STYLE TOOLS" and has two key objectives:

- To provide detailed examples of the use of the structural integrity assessment tools developed within STYLE in the context of ageing and lifetime management of pressure boundary/pressure circuit components
- To suggest best practice guidance for ageing and lifetime management of pressure circuit components at a European level

### **1.3 DESCRIPTION OF THE MAIN RESULTS**

The description of main S & T results reflects the thematic structure of the project, rather than strictly following the Work Package structure described in the previous chapter. Thus the following sections report the key activities surrounding each of the STYLE mock-ups, and the three major cross-cutting themes (weld residual stresses simulation and measurements, stress corrosion cracking and LBB).

#### **1.3.1 Narrow Gap Dissimilar Metal Weld Integrity - Large scale test on Mock-up 1 (MU1)**

MU1 was based upon an EPR type Alloy 52 narrow gap GTAW dissimilar metal weld between AISI 316L stainless steel and 18 MND 5 ferritic steel, identified as DMWinc. MU1 as provided by AREVA-NP France had a thickness of 40.5mm and an outer diameter of 352mm. This large scale mock-up was representative of a surge line in the EPR and corresponds to the scale ½ of the coolant primary circuit pipes linked to the reactor pressure vessel and of pipes connected to the steam generator. This mock-up was in the scope of a continuation of the ADIMEW project [1] and dealt with improvements in the assessments for DMW and Leak-before-break procedures.

The central part of the pipe had a through-wall circumferential EDM notch (Figure 1). Due to the very low angle of the narrow gap weld (2°), the crack plane put at the interface was in fact located at about 0.3mm from the interface in the Alloy 52 material on the outer surface and, at about 0.2mm

from interface in the clad ferritic steel on the inner surface. Two extension arms were welded to the central test section containing the DMW. The total length of the mock-up was about 7.8m. A chevron shape was machined. After the pre-cracking stage, the suitable two straight front lines were well obtained and formed the desired angle of  $2\beta = 90^\circ$ .

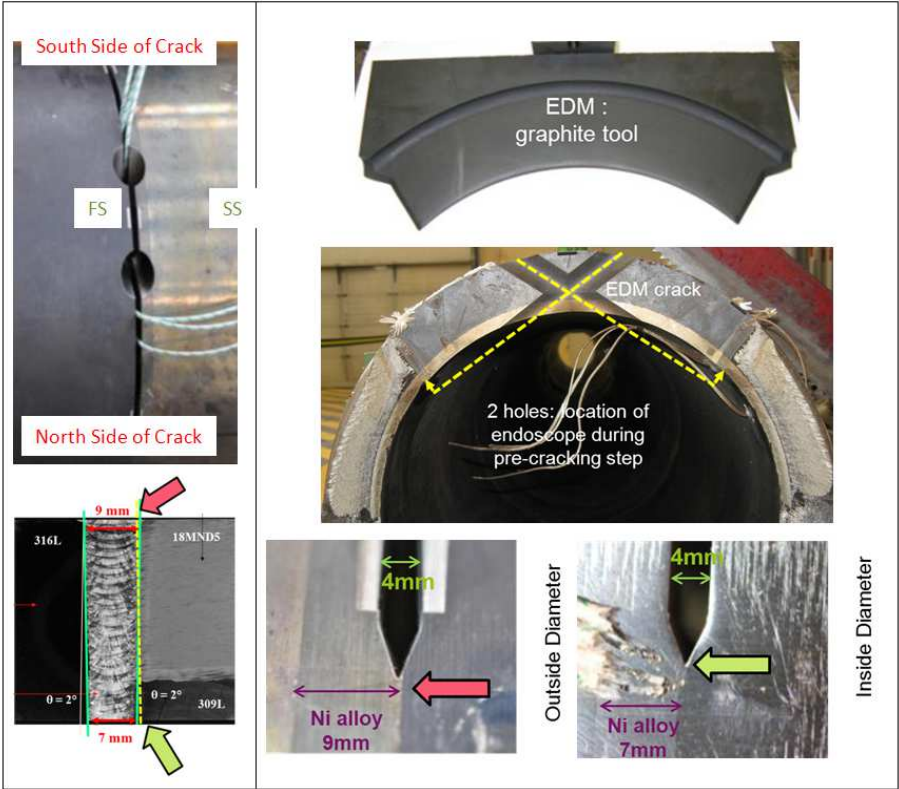


**Figure 1: Through wall defect on Mock-up 1: a) Machining of the V-shape, 2 holes for endoscopic observations inside the pipe and 3 clip gage grips, b) Crack located at the Alloy 52/ FS interface.**  
 The test was successfully performed in two steps (Figure 2). A maximum load of 435kN was reached corresponding to a value of 330mm of displacement. The test was performed in two steps due to the high value of displacement. The heating and cooling systems developed in order to achieve and maintain a homogenous temperature of 300°C in the central part of the mock-up during fracture test have been efficient. The temperatures are stable in the crack front area, gradients of temperature are low in the thickness (gap less than 7°C comparing outside and inside thermocouples) and along the pipe axis (between 270°C and 304°C).

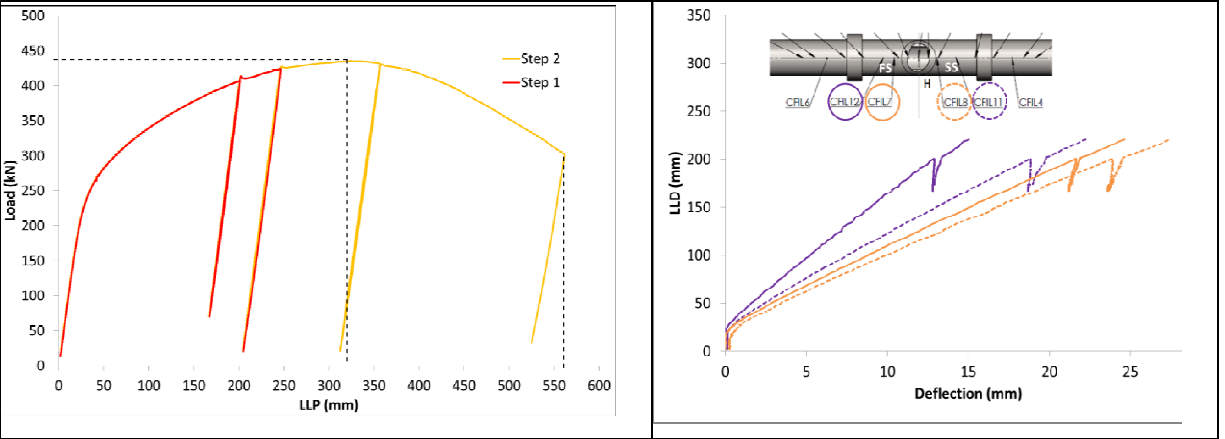


**Figure 2: Load vs LLP, Test in two steps, Deflections vs LLD along the DMW mock-up**

In the central DMW part of the extended mock-up, the deflection measurements show the unsymmetrical configuration of bending due to the difference of elasto-plastic properties between SS and FS (Figure 2). The CMOD are similar for the two clip gages in North and South sides, which means quite symmetrical crack propagation on both side of the through wall defect. The first non-linearity appears near 120kN on the clip gages curves (“global” plasticity). Only one unloading step is recorded with clip gages data, no significant variation of complaisance has been observed. The DDP measurement indicates a change of shape of the crack due to propagation and also other changes of geometry or non-linear phenomenon like plasticity.

In order to determine the crack initiation load, the relationship between deflector sensors and CMOD has been interpreted with the assumption that the relationship is linear until the crack is propagating. The slight modifications in the linear relationships gave indications when the crack is propagating. With the help of DDP measurement, the initiation load has been also estimated. Finally, surface crack observations are compared with estimated crack initiation load range. 375kN appears to be a quite reasonable estimated value. (Figure 3).

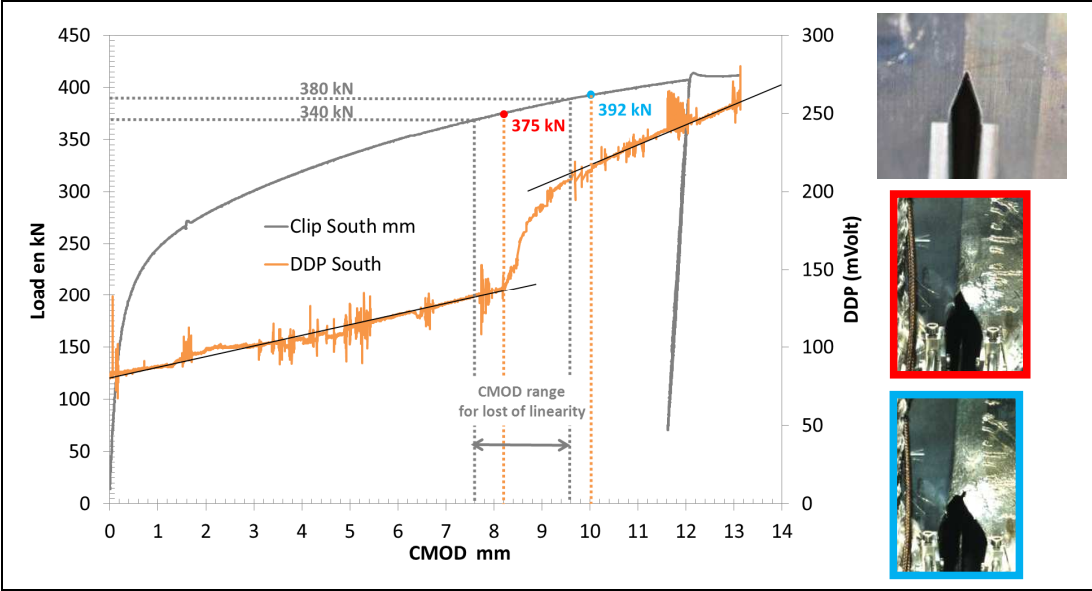


Figure 3: Evaluations of crack initiation load: Load, DDP versus CMOD and surface crack observation.

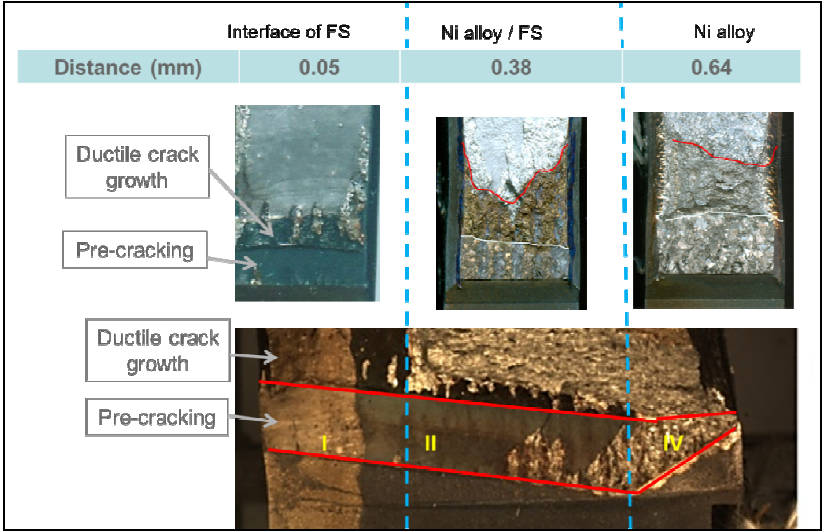
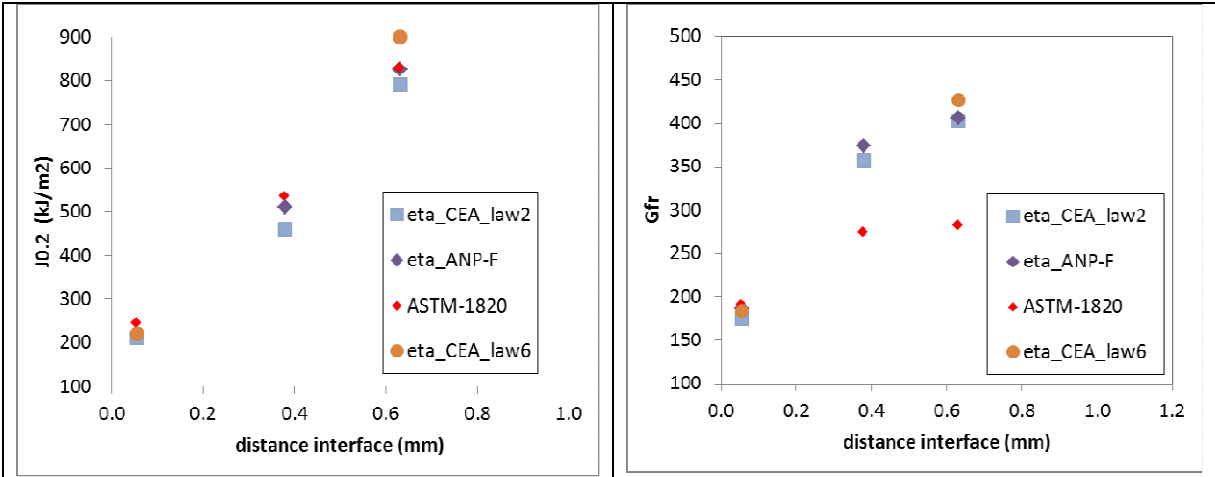


Figure 4: Comparison of the fracture surface of mock-up, with CT specimens: effect of crack distance.

Post-mortem investigations were done, a comparison of mock-up fracture surface was carried out with fracture surfaces on CT specimens (Figure 4). The crack stays in his fatigue pre-cracking plane when the crack is located at the interface FS/Alloy 52 (zone II). Nevertheless, the crack propagation by ductile tearing at the interface of FS/ Alloy 52 is restricted at about 2.5mm. When the distance between EDM crack plane and the interface is increasing (zone IV- distance 0.64mm on CT specimen), the crack is propagating only in alloy 52 and quickly is deviating to cross the weld thickness and to join the SS material; the resistance to ductile tearing is great. These observations are in accordance with the fracture properties analyzed on CT specimens (Figure 5).



**Figure 5:** Comparison of J0.2 and Gfr values, depending on the location of the crack relative to the interface, (data including FEM benchmark on corrected eta function).

After the first unloading step, the crack plane is deviating in the Alloy 52 very quickly at a load of 410kN. Between 410kN and the maximum of load of 435kN, the crack is located in the stainless steel. At the end of the test, a large propagation has been observed in the stainless steel material (Figure 6).

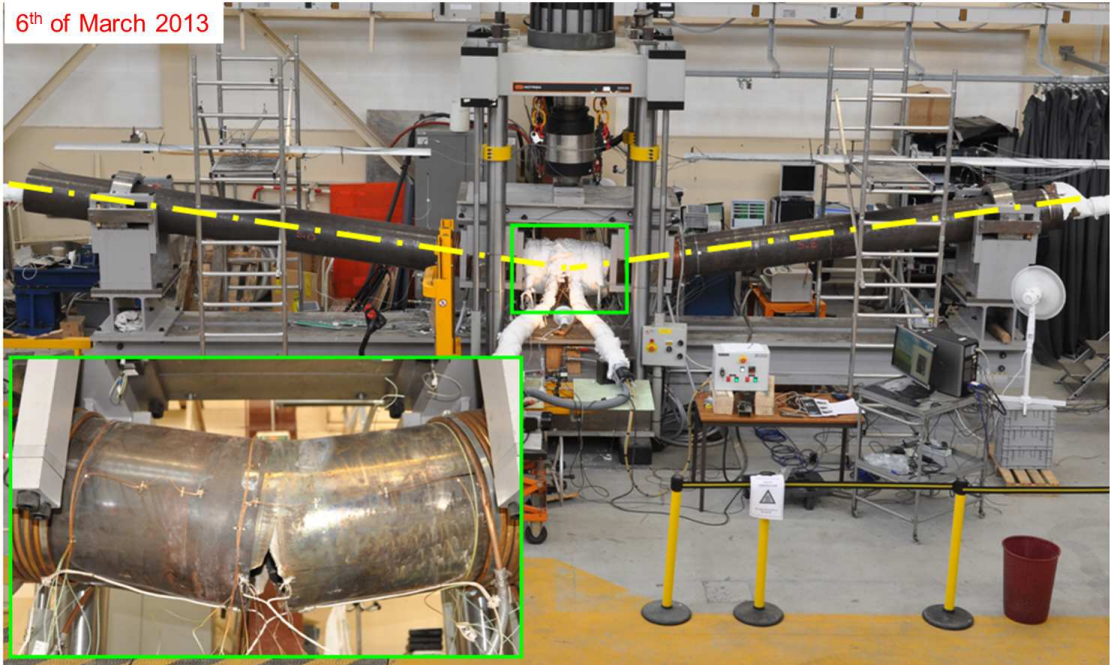


**Figure 6:** Fracture test: view of the South side of bending device at the end of step 2

### Fracture test interpretation by FEM: global approach

An analysis has been carried out by AREVA, and demonstrates that the J/G<sub>fr</sub> approach can be applied on a DMW. The analysis has shown the great effect of SS behavior law on the Load versus CMOD response. The test on base material has not been performed in axial direction. It was decided to add new tensile tests on specimens cut in the middle, in the bottom and in the top of the thickness of the pipe. The results have shown a gradient of elasto-plastic properties within the thickness, and the SS\_law1 had underestimated the three new stress-strain curves (Figure 7). New computations were performed with the new mean stress-strain law2 for the SS behavior at 300°C. The results were in very good accordance with the experiments (Figure 7). The calculations are undergoing in order to estimate the updated J value at initiation of the crack.

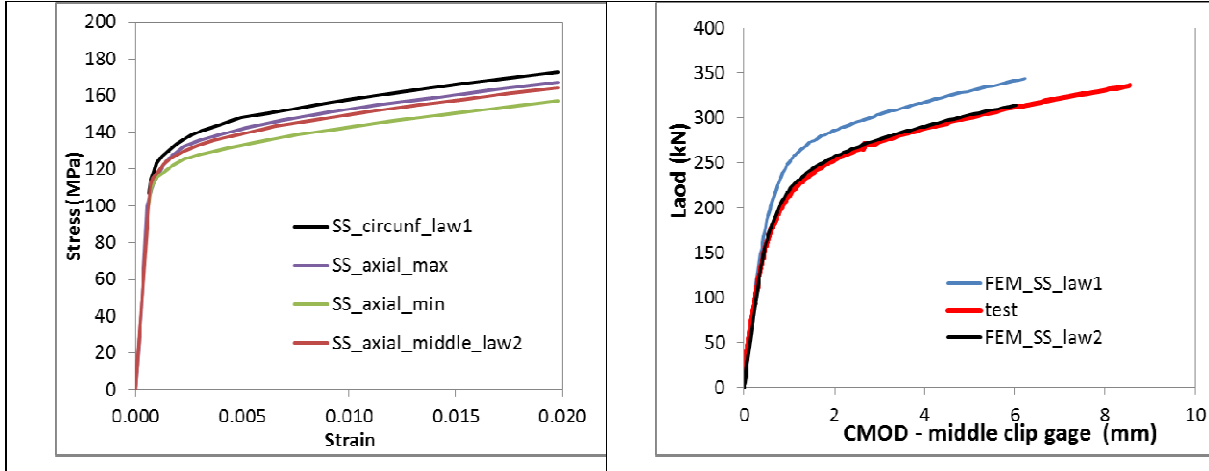


Figure 7: Load versus CMOD: comparison between test and F.E. depending on Stress-strain curves on SS base metal.

Achievements, lessons learned, and progress against STYLE objectives are:

- Detailed materials characterisation of all the constituents of a DMW is required to design and accurately interpret a large scale fracture test on a defect at the Alloy 52 to ferritic steel interface.
- The complexity of the material behaviour makes it necessary to interpret the characterisation tests using detailed finite element analysis.
- The MU1 large scale fracture test was successfully performed at a temperature of 300°C by applying four-point bending loading to a mock-up containing a circumferential through-wall crack nominally positioned at the Alloy 52 to ferritic steel interface.
- The test was extensively instrumented. In addition to actuator displacement and applied force measurement, the instrumentation consisted of 3 high temperature clip gauges attached to the mock-up at the centre of the crack and close to the each tip, 2 electric potential difference sensors (DDP measurement), 11 deflection sensors and 44 thermocouples.
- The post-test analysis indicated that crack initiation occurred at levels of the J-integral consistent with  $J_{0.2}$  measured in multi-material CT specimens.
- The global mock-up behaviour during the early stages of ductile tearing can be described using the  $G_{fr}$  criterion, based upon crack growth along the Alloy 52 to ferritic steel interface.
- Subsequent global behaviour is controlled by the limit load of the AISI 316 portion of the mock-up.



### **1.3.2 Effects of residual stress and thermal ageing on ductile fracture - Large scale test on Mock-up 2**

Welds made from austenitic stainless steels are not normally post-weld heat treated before entering service, so they will contain weld residual stresses of yield magnitude. The presence of high residual stresses has led to a number of ageing-related instances of in-service cracking in operating nuclear plant. Prominent, and costly, examples are high temperature creep cracking in heavy section AISI 316H welds in advanced gas cooled reactors (so-called reheat cracking), and primary water stress corrosion cracking in PWR primary circuit dissimilar metal welds made using Alloy 52 alloy 82 or 182. The presence of weld repairs exacerbates these problems, because the residual stresses in a weld repair are higher than in a plain girth weld, with both significant membrane stress components in weld longitudinal and transverse directions, and increased triaxiality.

Material ageing driven by prolonged high temperature exposure reduces the initiation toughness and ductile tearing resistance of austenitic materials. It is therefore possible to encounter conditions where ductile tearing could occur under conditions of small scale yielding or well-contained yielding. Here assessment procedures such as R6, and explicit J-integral estimates, both predict that residual stresses will impact crack initiation and growth.

Designing validation tests to underwrite or dismiss such predictions is extremely difficult, since they must combine high residual stresses with relatively low ductile tearing resistance, and crack initiation and growth must take place under conditions of small-scale and contained yielding.

The STYLE MU2 test was designed to achieve these conditions, by combining high repair-weld residual stresses with ductile tearing resistance low enough to expect crack initiation and growth in conditions of limited primary load induced plasticity. The predictions made by R6, conventional cracked body analyses, and ductile damage models could then be tested against observed behaviour in a loading regime where generalised plasticity had not reduced the predicted impact of residual stress to levels hidden by experimental scatter. The test would also provide a benchmark for the assessment of LBB methods, and the mock-up itself a valuable case-study for the prediction and measurement of weld residual stresses.

The MU2 test was originally intended to be performed on aged material. Austenitic weld metal and castings often contain delta-ferrite. High temperature exposure of these materials can cause large falls in the fracture toughness and an increase in the yield strength. The same high temperature exposure also causes relaxation of the as-welded residual stresses due to creep. However, in austenitic steels at AGR steam temperatures this relaxation is never complete, so significant stresses remain.

In the event, the impact of the chosen accelerated ageing conditions on the fracture toughness of the chosen austenitic weld metal was so severe that the material became macroscopically brittle, with a very low fracture toughness. The same high temperature exposure reduced the residual stresses, but sufficient remained to have two effects. First the large scale test would involve sudden brittle fracture of the entire mock-up under small-scale yielding conditions where the impact of residual stress is already well understood – there would be no advance in the state of the art. Second, it was judged likely that the mock-up would fail during fatigue pre-cracking due to the combined effects of residual stress and low toughness. This was deemed unnecessarily risky, so the aged MU2 mock-up was replaced with an identical but unaged equivalent. The repair weld residual stresses in this mock-up were at a very high level. The weld material was fully ductile, but also had high yield strength, meaning that crack initiation and ductile tearing were predicted to occur in small scale yielding conditions, with residual stresses having a large effect on the crack initiation load.

MU2 was based around a thick-walled pipe section, of total length 600mm, wall thickness 35mm and outer diameter 180mm, containing a central J-preparation girth weld with a short, deep weld repair. The test pieces were manufactured from Esshete 1250, an austenitic stainless steel with added vanadium and niobium to increase its strength at high temperature, which is used for AGR boiler support structures operating at temperatures up to 580°C. Both the girth and repair welds were made

with matching weld consumables using manual metal arc (MMA) techniques. A completed mock-up is shown in Figure 8.

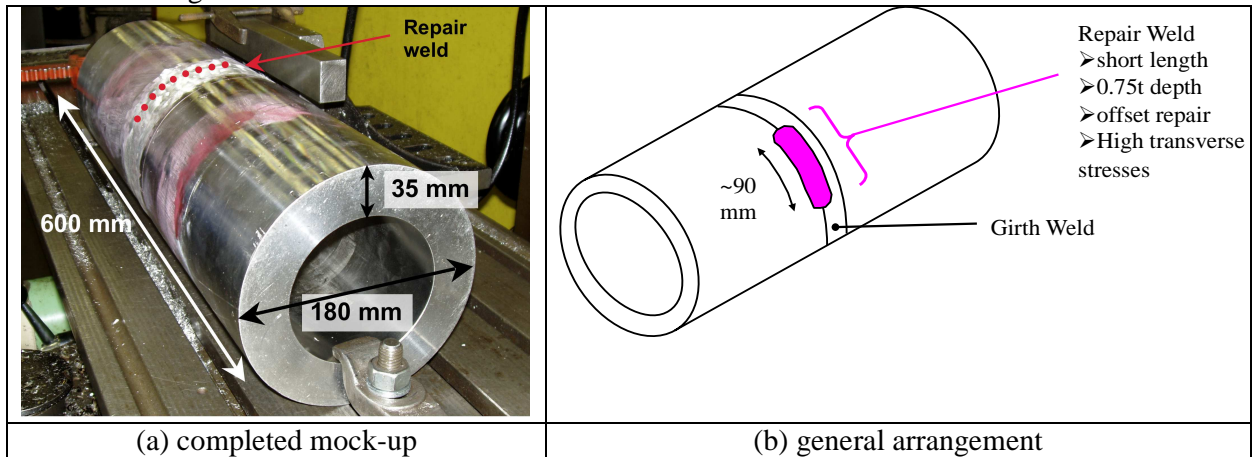


Figure 8: STYLE Mock-up 2

A chevron starter notch was then inserted into the mock-up at the centre of the weld repair using specially designed EDM tools, and making use of the circular hole left at the repair centre by the prior iDHD measurement. The notch profile was chosen to ensure fatigue pre-cracking resulted in a radial final crack front, despite the large gradient of primary stress intensity factor through the pipe wall caused by the combination of global bending loading and low R/t. The notch geometry is shown in Figure 9.

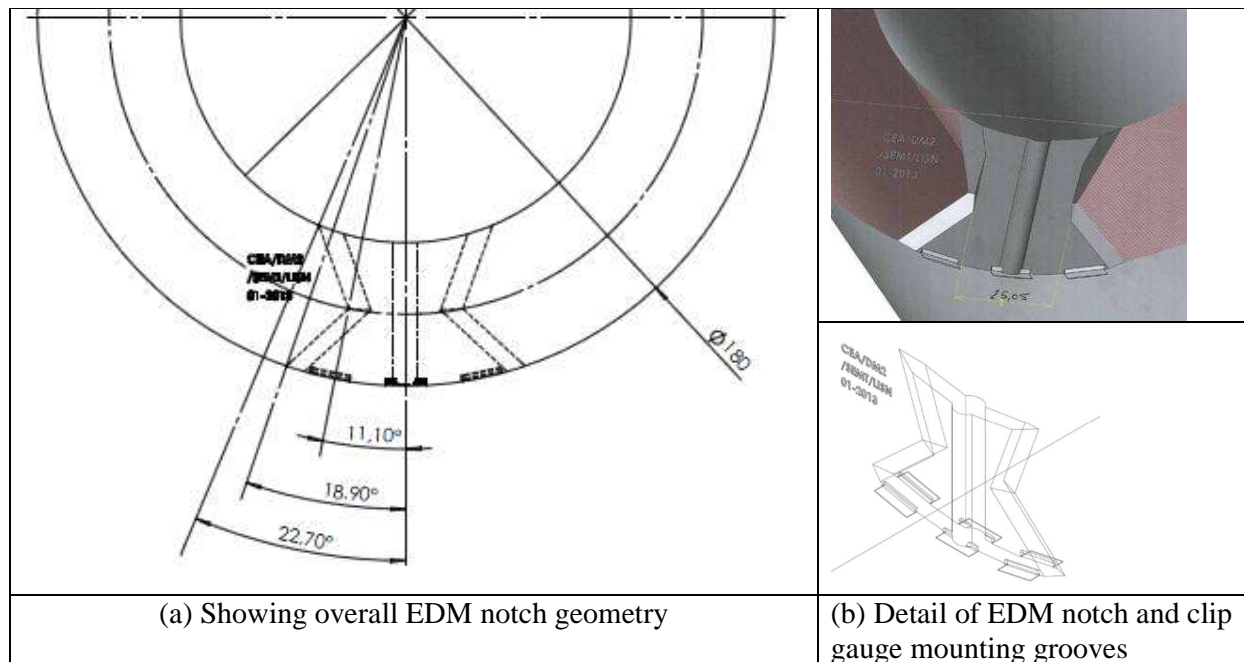


Figure 9: EDM pre-fatigue notch inserted into Mock-up 2

The MU2 test was performed on 19<sup>th</sup> June 2013. The mock-up was instrumented with two clip gauges recording CMOD at the outer surface for the two crack tips, and dc potential drop equipment at the two outer surface crack tips, see Figure 10.

The specimen was loaded under displacement control. Loading was interrupted at intervals and the specimen unloaded both to record the elastic compliance at the CMOD gauges, and hopefully to mark the fracture surface, thereby providing further information on crack growth.

Significant crack tip deformation was observed during the test, although it proved difficult to visually distinguish between crack tip blunting and ductile tearing. The test was stopped after achieving a peak load of 213.1kN at a ram displacement of 242mm.

After the test was complete, the crack was extended using fatigue loading, and the fracture surfaces removed for fractographic examination.

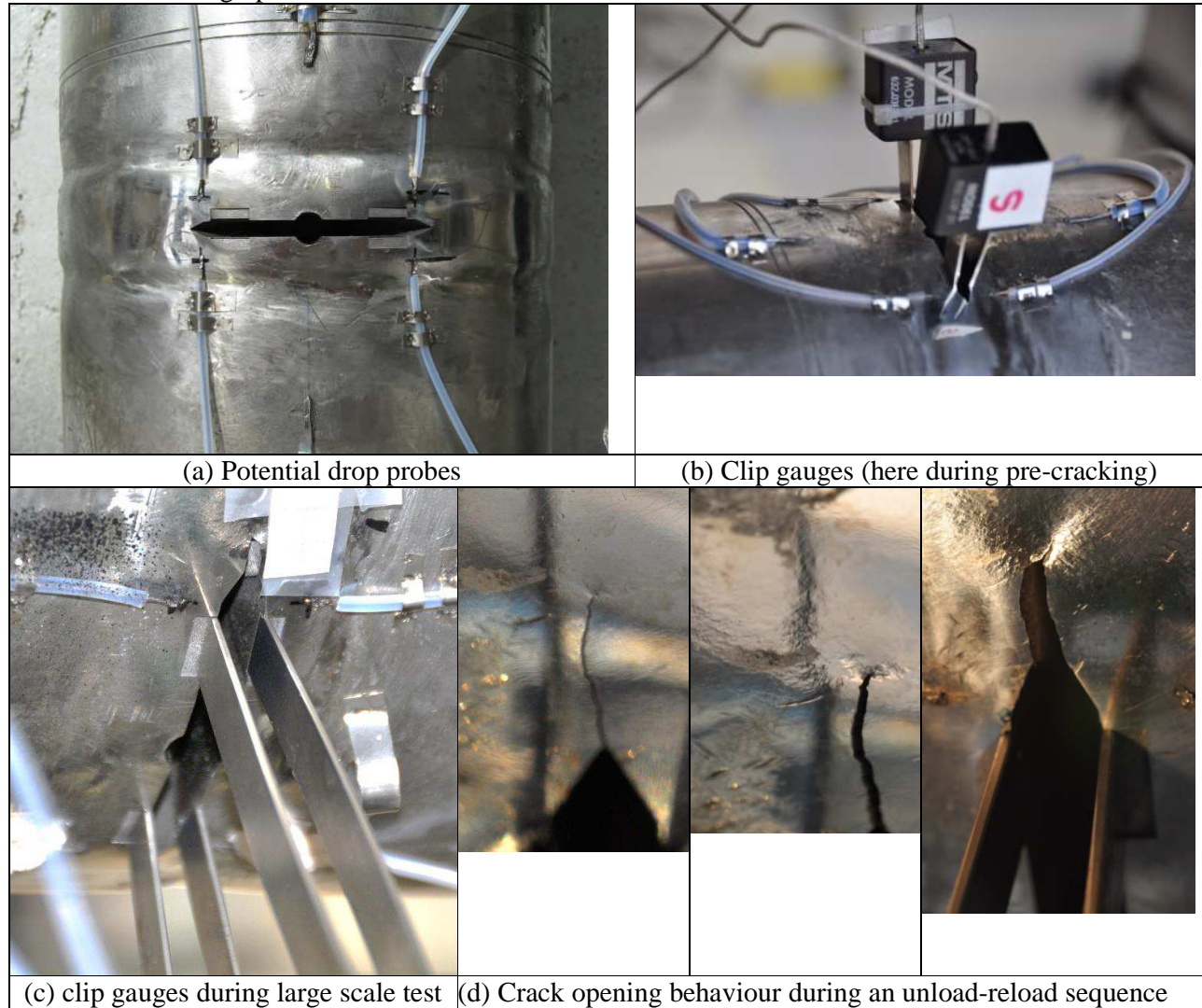


**Figure 10: Mock-up 2 test instrumentation, and crack opening behaviour during an unload-reload cycle**

The global load displacement response measured during the test is compared with the final test prediction in Figure 11. There are two obvious observations:

- 1) Global non-linearity was observed much sooner during the test than predicted. The reasons for this are not yet clear. Visual observation of the deformed shape of the pipe during testing suggested that plastic deformation occurred at the attachment welds between the central Essete pipe and the AISI 304 extensions. This observation needs to be underwritten by detailed post-test analysis of the measured deformations along the mock-up (rather than the ram displacement, which is remote from the pipe load points).

- 2) The peak load achieved, 213kN, is lower than the crack initiation load predicted using primary load alone. Thus if crack growth occurred during the test, it must have been strongly influenced by the weld residual stresses.

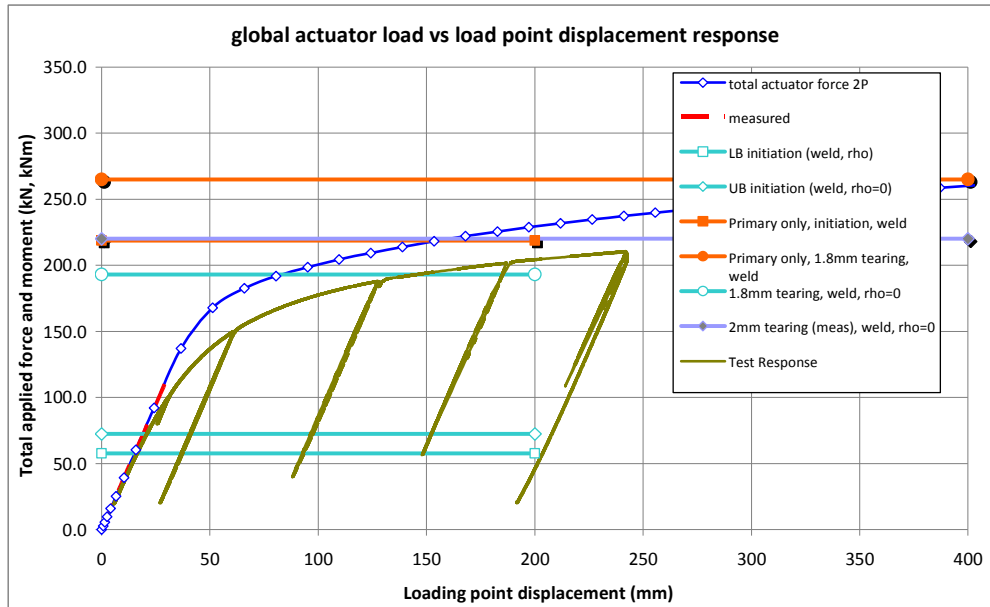


**Figure 11: Predicted load vs. load point response compared with measured load vs. ram displacement response for Mock-up 2 test**

Achievements, lessons learned, and progress against STYLE objectives:

The MU2 test design criteria were:

- The material should be ductile (rising  $J-\Delta a$  curve).
- The yield strength should be high, to delay plastic re-distribution of the residual stresses.
- The residual stress measurements should be reliable and diverse.
- The residual stresses should be high and relatively uniform across the test defect.
- R6 should predict crack initiation at  $L_r < 0.5$  (SSY conditions).
- The predicted initiation ratio with/without residual stress should be as large as possible.
- The test should reach 2mm of ductile tearing in contained yielding conditions.

The MU2 experiment achieved all these objectives. Up to 3mm of stable ductile tearing was observed at loads below the predicted initiation load for primary load alone. Despite the delays caused by changes to the material condition selected for testing, overall the test was a significant achievement.

### 1.3.3 Transferability in Clad pipes - Large scale test on Mock-up 3 (MU3)

Usually, material data necessary for fracture mechanic analyses are obtained by testing small specimens, which are subsequently used for the assessment of large scale structures (real components). This approach is believed to be conservative since the material fracture properties are obtained on highly constrained standard compact tension (CT) specimens. The strategy followed in STYLE is to investigate the influence of specimen size, crack shape and type of loading on fracture mechanics properties like crack initiation load and amount of crack growth.

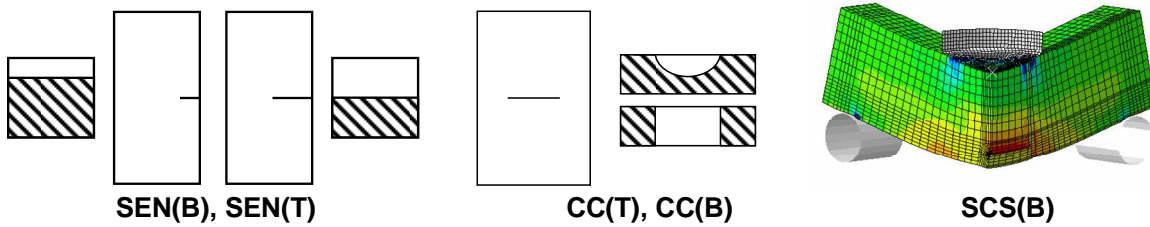


**Figure 12: Constraint modified specimens**

The experimental programme on constraint modified specimens consisted of uniaxial and biaxial small scale specimens with different crack shapes and  $a/W$  ratios (see Figure 12). Additionally tests on standard specimens were performed in order to obtain material properties for design and post-test analyses of MU3. The crack orientation for all small scale specimens was the same as the orientation of the initial crack in MU3.

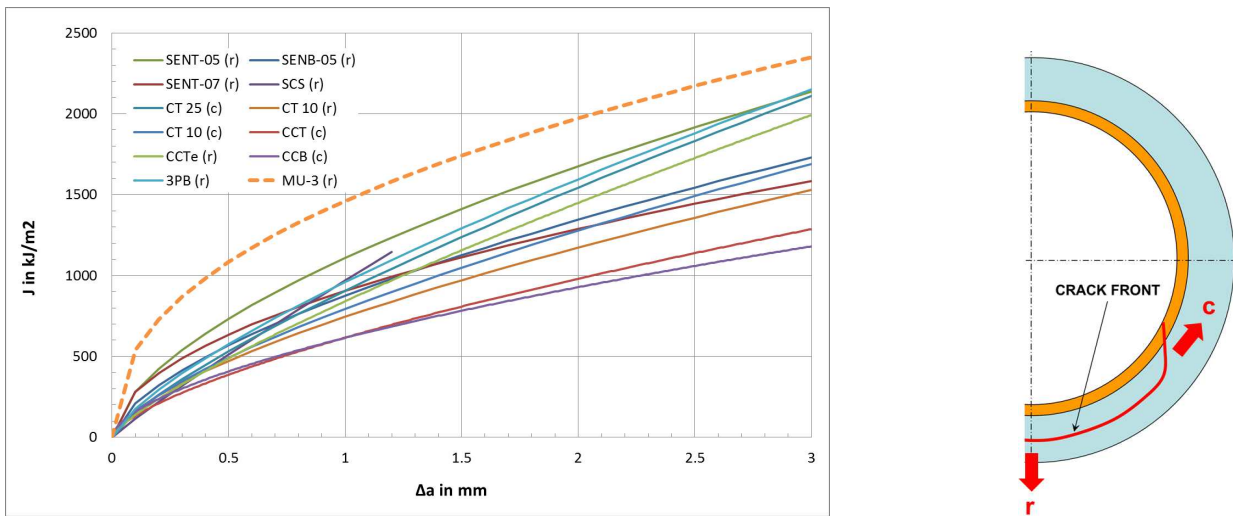


**Figure 13: Resulting  $J$ - $\Delta a$  curves and direction of crack propagation in small scale specimens (Mock-up 3)**

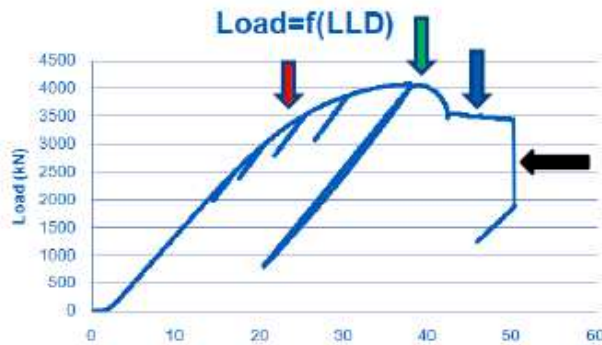
Figure 13 shows the resulting fracture resistance curves ( $J$ - $\Delta a$  curves) obtained by testing different standard and non-standard specimens and MU3. The specimens' orientation (crack propagation directions) related to MU3 is identified as (c) for the crack propagation in the pipe's circumferential direction and (r) for the crack propagation in the radial direction (through-wall).

To be on the safe side, the conventional fracture mechanics assessment (using the  $J$ -Integral as single parameter) is based on lower bound toughness from highly constrained specimens, typically CT or SEN(B). It can be seen that  $J$ - $\Delta a$  curves obtained by testing small scale specimens with deep cracks are conservative (they have considerably lower fracture toughness) for the fracture mechanics assessment of large scale components (compare with  $J$ - $\Delta a$  curve of MU3). The experiments on small scale specimens have also shown that crack initiation in the ductile regime is rather independent of the crack constraint and that a biaxial loading does not significantly influence the crack initiation and crack propagation.

The MU3 experiment was performed on 13th March 2012 at room temperature under ram displacement control (see Figure 14), with several unloadings during the test (see Figure 15), four partial unloading (20 % unloading) and a last more significant unloading (80 %).



Figure 14: View of Mock-up 3 during the test



0	Yielding
1	Ductile tearing initiation
2	Ductile tearing in radial direction (through wall thickness)
3	Ductile tearing in circumferential direction
4	Cleavage initiation, propagation and arrest
5	End of test

Figure 15: MU3 Load vs. LLD

The test proved to be very successful with the detection of crack growth initiation occurring near the deepest point of the flaw (~3500kN). Significant ductile tearing crack growth was evident, first in the radial and then in the circumferential directions followed by the final instability (cleavage) with significant brittle propagation and arrest, without full failure of the pipe.

Figure 16 shows the comparison of the post-test analysis with the experimental results (CMOD vs. Load). The predicted crack initiation is 3800kN, which is somewhat higher than the measured crack initiation by electrical potential drop method. This deviation is probably caused by a relatively coarse finite element mesh (average element size is 0.3mm). A better agreement would be possible by using smaller elements (0.2 or 0.1mm). The price however would be a substantially longer calculation time.

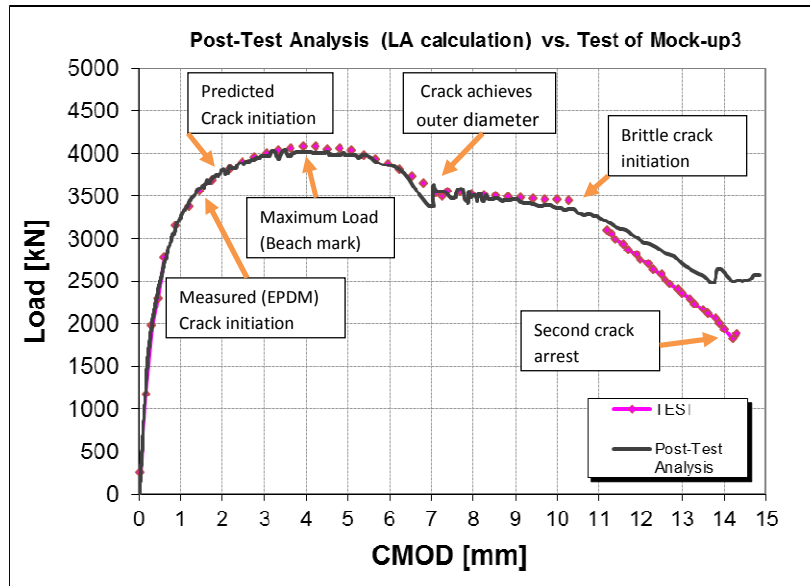
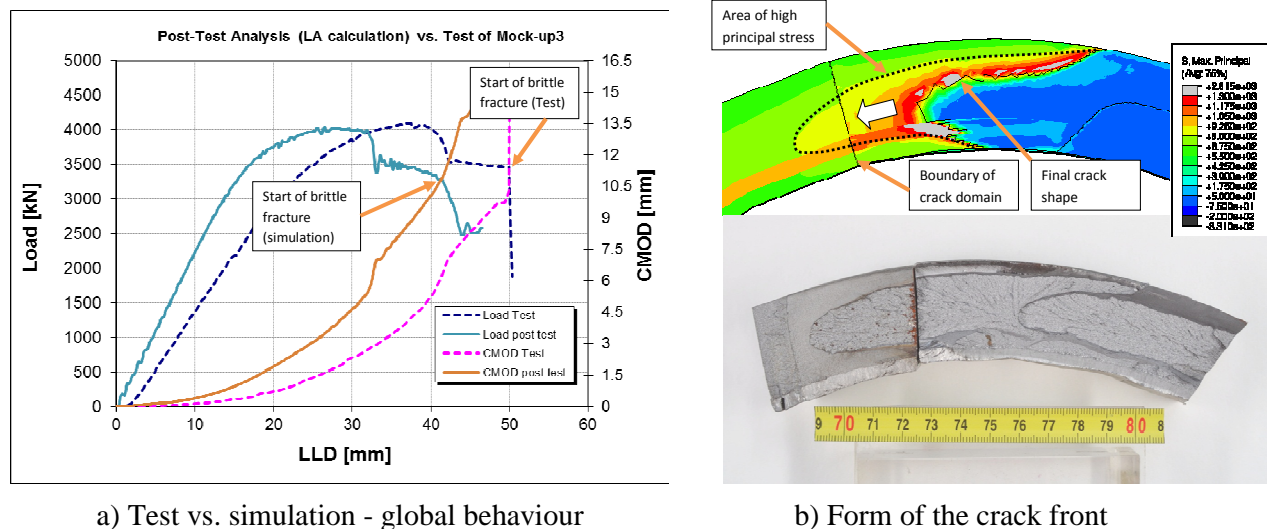


Figure 16: A comparison of the post-test analysis with the test (Mock-up 3)

The last stage of the MU3 test, the final brittle fracture, cannot be described accurately by the applied micromechanical model. However, interestingly, the results of the post-test analysis show a drop in the reaction force at the time of the brittle initiation (see the comparison in Figure 17a). The following crack propagation is considerably slower than that observed for brittle fracture at the end of the test. Nevertheless a qualitative statement about the expected crack form, propagation direction and stress distribution can be given.



a) Test vs. simulation - global behaviour

b) Form of the crack front

Figure 17: Crack propagation: post-test analysis vs. experiment (Mock-up 3)

Figure 17b shows a comparison of crack shape at the end of the test with the result of the local approach simulation. It can be seen that the final crack shape at the end of simulation has a similar form to that observed in the test (compare with the crack shape developed at the end of the test). Moreover the high principal stress emerging in front of the simulated crack shape indicates quite accurately the form and direction of further (unstable) crack propagation. Hence the simulation confirms the trends effect observed in the test (in particular the crack propagation inside the wall described as “tunnelling”).

Achievements, lessons learned, and progress against STYLE objectives:

In summary it has been shown that the classical global approaches like J-  $\Delta a$  or plastic limit load lead to conservative prediction of the large scale test outcome. If J-  $\Delta a$  predictions are made it is recommended to use J-  $\Delta a$  curves obtained from standard CT specimens. In this case even a large extrapolation of ductile crack growth gives conservative results.

The crack growth simulation based on the modified Gurson local approach method constitutes a valuable help in both design and post-test (interpretation) phases and provides quite accurate information in terms of the real crack growth extent and the limit load of the component respectively. The micromechanical material model applied in this work is particularly suitable for simulation of ductile tearing problems. However, some limitations occur in cases where there is a smooth transition from ductile to brittle fracture regime. Because of the complexity of the local approach methods, experience is necessary in the correct application. To facilitate the broader use of these advanced methods to complex assessments it is recommended that adequate benchmarks and training should be performed.

Regarding the transferability of material properties in structural integrity assessment it was confirmed that J- $\Delta a$  curves obtained by testing small scale specimens with deep cracks are conservative for the fracture mechanics assessment of large scale components. The experiments on small scale specimens have shown that crack initiation in ductile regime is rather independent of the crack constraint and that a biaxial loading does not significantly influence the crack initiation and crack propagation.

#### **1.3.4 Weld residual stress simulation and measurement (MU4 results)**

(Because of prescribed limitations on the length of this report only residual stress result related to the MU4 are presented in this chapter. However similar work has been undertaken for other STYLE mock-ups: MU1, MU2 and MU6)

The objectives were as follows:

- Provide data on welding residual stresses for mock-up assessment.
- Collect data for validation of the WP2 activities on welding residual stress prediction.
- Undertake weld simulations to predict as-welded residual stresses for comparison with measurements in girth welded pipes.

MU4 comprised four stainless steel pipe welds, 2 pipes manufactured using low heat input and two with high heat input, all provided by IdS. For each heat input one pipe had a weld repair introduced.

The results of residual stress measurements associated with MU4 are confined to samples MU4-1 and MU4-2. Both these as-welded pipes were measured using deep hole drilling through the centre of the weld. Measurements were also made using neutron diffraction and the contour method. Results from MU4-1 are shown in Figure 18 and illustrate that all three measurement methods produced similar trends in the distribution of the residual stresses. However, the details obtained from each technique are different.

Both DHD measurements on MU4-1 and MU4-2 pipes, illustrated in Figure 19 show a typical sinusoidal distribution of a welding residual stresses from outer weld surface. This means that from the outer weld surface, both hoop and axial stress start in tension, decreasing to compression near the inner weld surface. The results show that the average of membrane residual stresses was increased to about 150MPa by the presence of the repair weld.



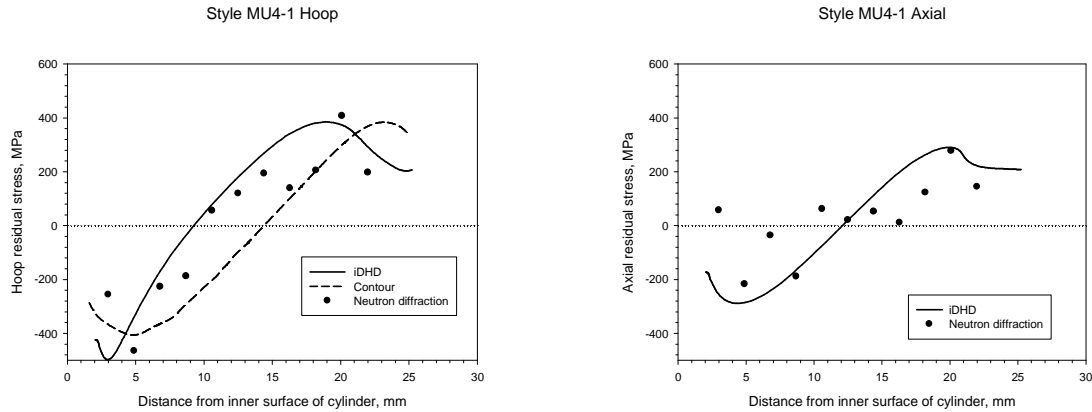


**Figure 18: Measured through-wall residual stresses in an as-welded stainless steel girth weld**

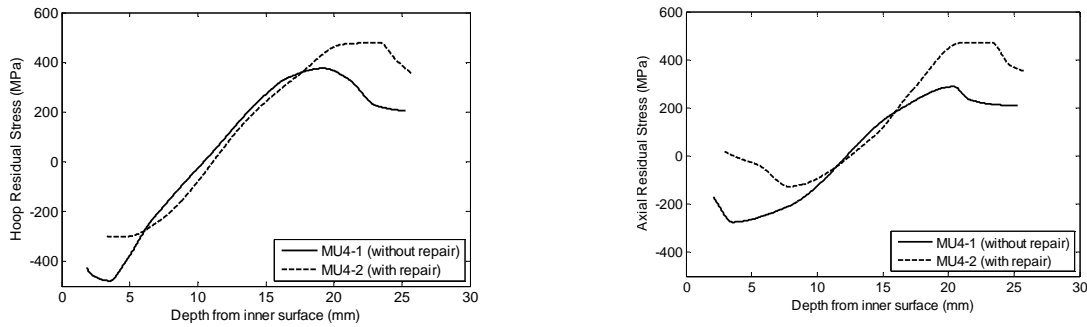


**Figure 19: Measured through-wall residual stresses in as-welded and repair welded stainless steel girth welds (Mock-up 4)**

The MU4 pipe girth welds were made in AISI 316L using a mechanised TIG technique. A wide weld preparation with a backing plate was used, and the welds were made with two different heat input levels. Figure 20 gives details of the overall mock-up layout and the weld pass sequence for MU4-1, a low heat input girth weld. MU4 differed from the short girth-welded pipes primarily in the weld preparation design, which resulted in significant distortion during welding. Figure 21(a) shows that the final weld was only 11mm wide at the root, compared with an original preparation width of 20mm. Note that the simulations reported here used the original weld geometry, so modelled a final weld that was too wide.

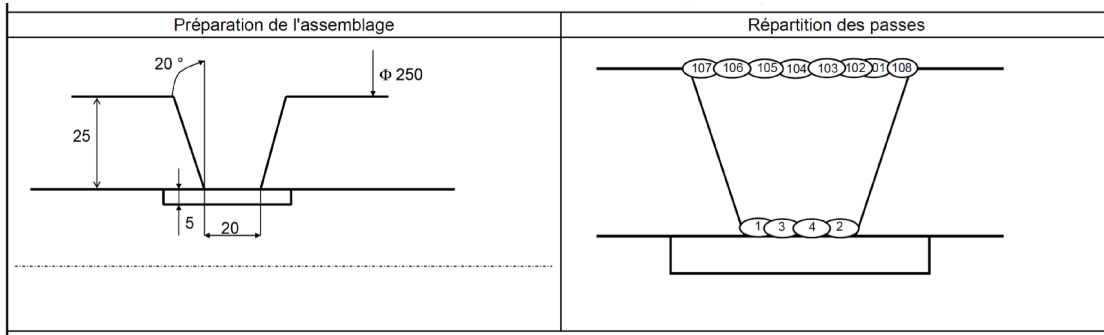
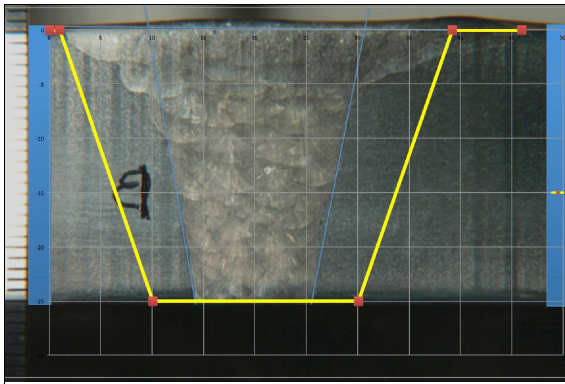


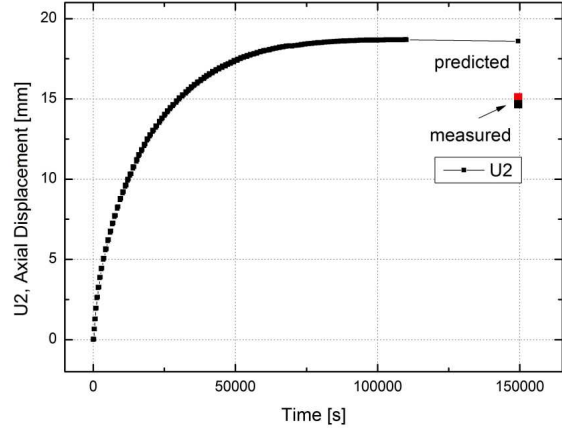
**Figure 20: General layout, weld preparation design, and weld pass sequence for mock-up MU4-1**

The simulations performed on the MU4 girth welds followed exactly the same approach used successfully for the MU2 welds presented above. It was found that the axial restraint imposed on the model during welding was a significant analysis variable – the correct axial contraction was only achieved by preventing axial expansion during welding (see Figure 21(b)). Radial contraction at the weld remained slightly under-predicted, see Figure 21(c).

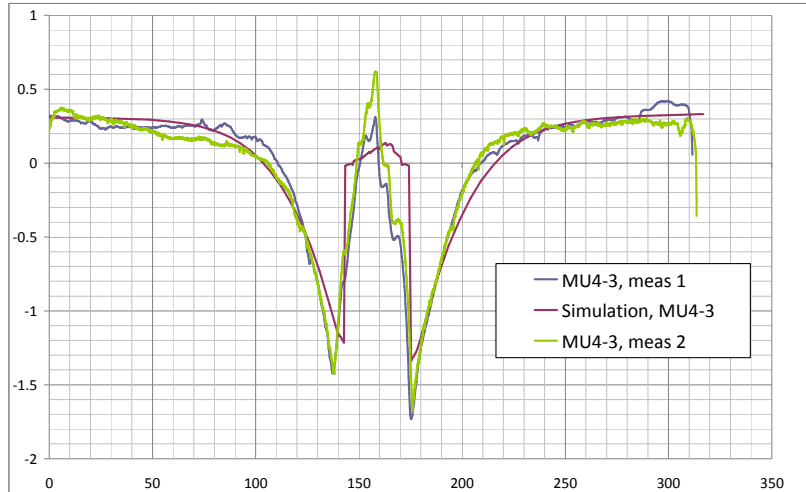
Comparisons of predicted and measured residual stresses showed broad agreement in the hoop direction (see the MU4-1 results in Figure 22(a)), although the peak stresses were under-predicted. Stresses in this direction are normally most sensitive to the material hardening model and the assumed yield stress. In this case, the material properties are considered to be correct, since the materials are the same as those used in NeT TG4. It is believed that the under-prediction is associated with modelling an over-wide weld geometry. In the axial direction (see Figure 22(b)) agreement is relatively poor, even when axial restraint is employed. Weld transverse stresses in girth welds are relatively insensitive to the material hardening behaviour, and it is judged that the poor agreement is due to differences between the FE models and the actual weld geometry.



(a) transverse weld macrograph compared with original weld preparation for MU4-1

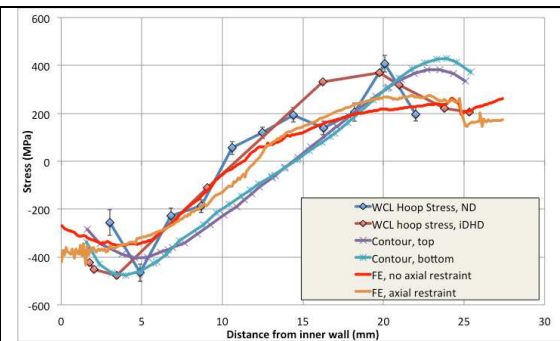


(b) Predicted and measured transverse (axial) contraction (U2) across weld in MU4-1

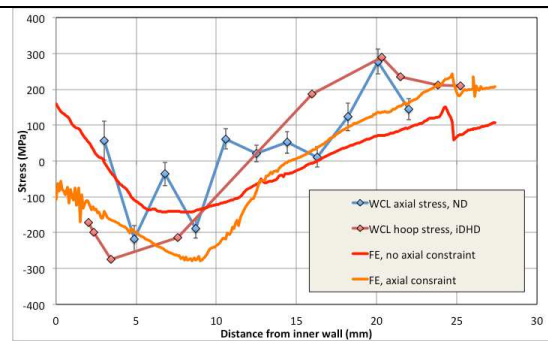


(c) Predicted and measured radial profile for MU4-3 (axes in mm)

**Figure 21: Comparing completed weld cross-section with original weld preparation, comparing predicted and measured axial contraction, and predicted and measured radial contraction, for MU4 girth welds**



(a) Hoop (weld longitudinal) direction



(b) Axial (weld transverse) direction

**Figure 22: Comparing predicted and measured hoop (left) and axial (right) residual stresses at weld centreline of mock-up MU4-1**

Achievements, lessons learned, and progress against STYLE objectives:

The measurements performed on plain girth welds and weld repairs were made using diverse methods, and provide valuable additional data on residual stresses in these welds. Because they were made using diverse modern techniques, they provide an important supplement to historical data, much of which was obtained using less capable and less diverse techniques.

The residual stress simulations showed that accurate predictions of residual stresses in conventional austenitic plain girth welds can readily be achieved if the simulations are controlled by detailed protocols and if appropriate mixed isotropic-kinematic material hardening is used.

Where welding distortion is significant, it is more difficult to obtain accurate predicted stresses, and the simulations must incorporate details of the actual weld profiles. Axi-symmetric simulations must be restrained against axial expansion during welding.

### **1.3.5 Stress Corrosion Cracking**

Due to the ability of Ni-based alloys to offer good mechanical properties, corrosion resistance and compatibility to other materials, Alloy 182 is frequently used as weld metal for internal components of PWRs. However a significant number of investigations have shown that Ni-based alloys are susceptible to Primary Water Stress Corrosion Cracking (PWSCC). This phenomenon is responsible for the structural damage and macroscopic failure of certain reactor components. One mitigation technique for PWSCC is the application of weld overlay. Weld overlays of Alloy 52 are believed to possess excellent stress corrosion cracking resistance due to their higher Cr content and are typically applied over susceptible dissimilar metal welds, like Alloy 182, with the expectation that they will act as a barrier to SCC.

For life-time prediction it is important to ascertain the time-to-failure for a given stress and environment. Generally, the time-to-failure due to stress corrosion cracking consists of three parts: (1) incubation-precursor stage, (2) crack initiation and (3) crack propagation. Final mechanical fracture will occur due to overload of the remaining cross section of the component.

The research work has been focused on crack initiation and crack growth rate tests of an industrially produced narrow gap Alloy 52 weld.

The different corrosion tests should reveal whether this material is susceptible to stress corrosion cracking in the given environment or not. A possible outcome of this study can be that the material has a high resistance to stress corrosion cracking (not susceptible at all). If there is a certain susceptibility to stress corrosion cracking, crack growth rates and crack initiation tests ( $\approx$  time-to-failure tests) should reveal the boundary conditions under which the material can be used.

The experimental results obtained in WP1.4 have been transferred to WP2.3 Stress Corrosion Cracking modelling to support the models developed there. Alloy 52 has however a high resistance to stress corrosion cracking. That means that the experimental data are difficult to use for an empirical model. Therefore the modelling work is focussed on Alloy 182, for which a lot of data are available. Empirical laws for crack growth (like MRP-115) and crack initiation (Win-PRAISE07 and xLPR) for this material are available as well. The models for Alloy 182 can then be transferred to Alloy 52 models with so called "improvement factors". With these "improvement factors" an engineering curve like a crack growth rate law can be decreased. For instance the crack growth rate of Alloy 52 can be up to a factor of 100 lower than the crack growth rate of Alloy 182 under similar conditions.

So at the end of the project these "improvement factors" would be determined from the experimental data and transferred to WP2.3 Stress Corrosion Cracking modelling, where they could be used to adjust/modify some of the existing models for SCC.

In addition, a crack growth rate model for Ni-based alloys in a PWR-relevant environment has been proposed and applied to Alloy 600. It belongs to the class of film-rupture/dissolution/re-passivation

models. However, the lack of data on experimental conditions related to published crack growth rate data meant that the model is not fully parameterized as yet.

Corrosion tests have been carried out under simulated PWR primary water conditions. That relates to a test temperature between 300 – 340°C, a pressure of 150bar and well-conditioned feed water (high purity water with addition of Li, B and hydrogen). Commonly used water chemistry is 2 ppm Li, 1000 ppm B and 30 cc/kg dissolved hydrogen. Such tests are typically carried out with a water recirculation loop connected to an autoclave. A schematic is shown in Figure 23. The water is prepared and then stored in the storage tank. From the storage tank the water is fed to the autoclave by a high pressure pump. The water is heated up using a pre-heater and heater around the autoclave. After the autoclave the water is cooled down and passes a back pressure regulator before it is fed back to the storage tank. The low temperature, low pressure part of the loop contains sensors to measure the water chemistry of the inlet and outlet water. Most laboratories measure the pH, conductivity, oxygen concentration and dissolved hydrogen concentration of the water. An ion exchanger (pre saturated with the Li and B concentration of the feed water) cleans the water before it re-enters the storage tank.

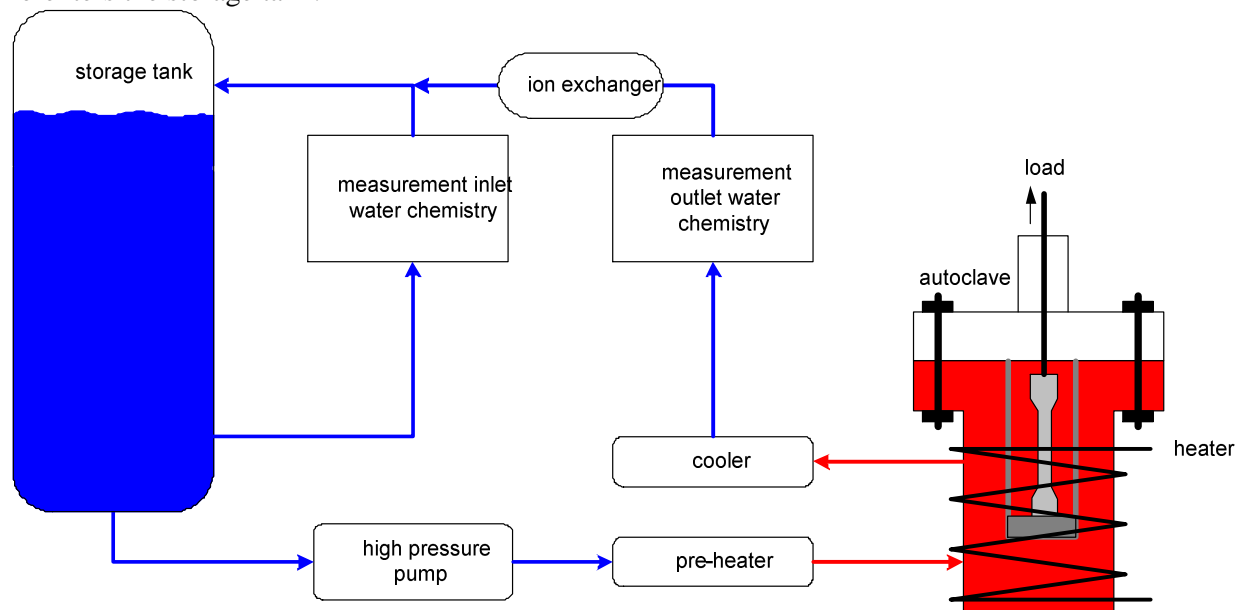


**Figure 23: Schematic of a water recirculation loop and autoclave for SCC testing**

In the autoclave a loading rig is installed to carry out the mechanical tests. Experimental techniques will be carried according to ASTM standards and/or international guidelines, where available.

The SSRT tests showed that Alloy 52 has a high resistance to SCC in PWR water. An example of a result at 340°C is shown in Figure 24. There is no difference in strain to-failure between the test in PWR water and argon. This has been confirmed by the SEM pictures of the fracture surfaces of the tensile specimens.

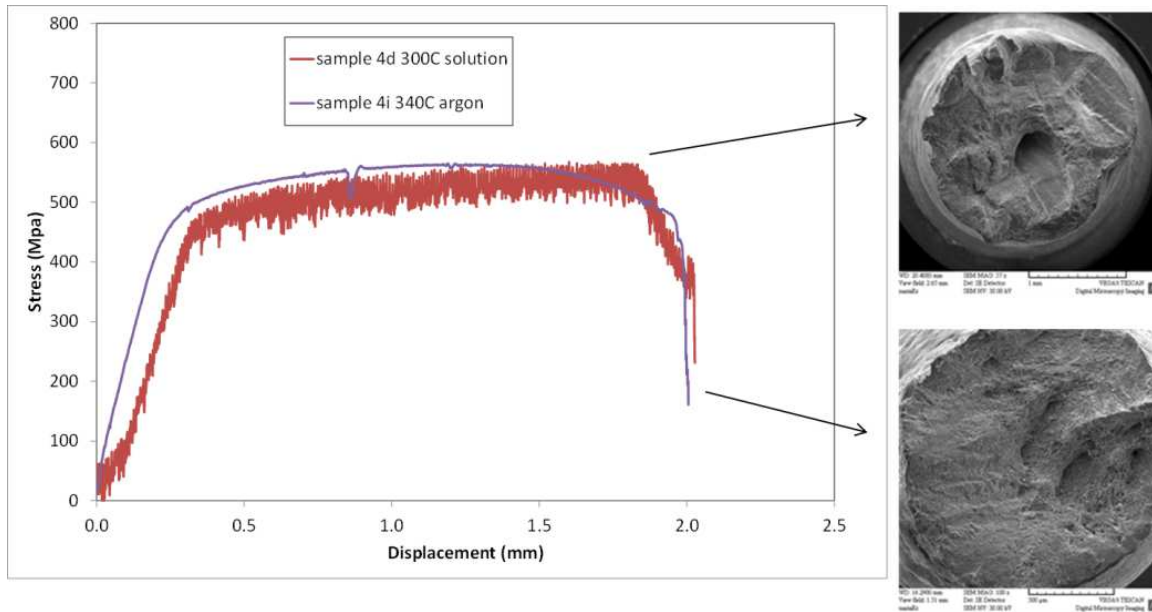


**Figure 24: SSRT test results of Alloy 52 in PWR environment and argon**

Crack growth rate tests were carried out with small size DCTs. One example is shown in Figure 25. As only part of the DCT is made out of Alloy 52, it happens that the SCC crack started in the base metal (carbon steel) and then entered the Alloy 52 after some time. However for none of the specimens, was there a measurable crack growth rate. To deal with this, we set an upper limit for the crack growth rate, based on the resolution of the test equipment and test time. In this way, a typical crack growth rate of  $\leq 10^{-9}$  mm/s ( $\approx \leq 0.03$  mm/year) could be defined.

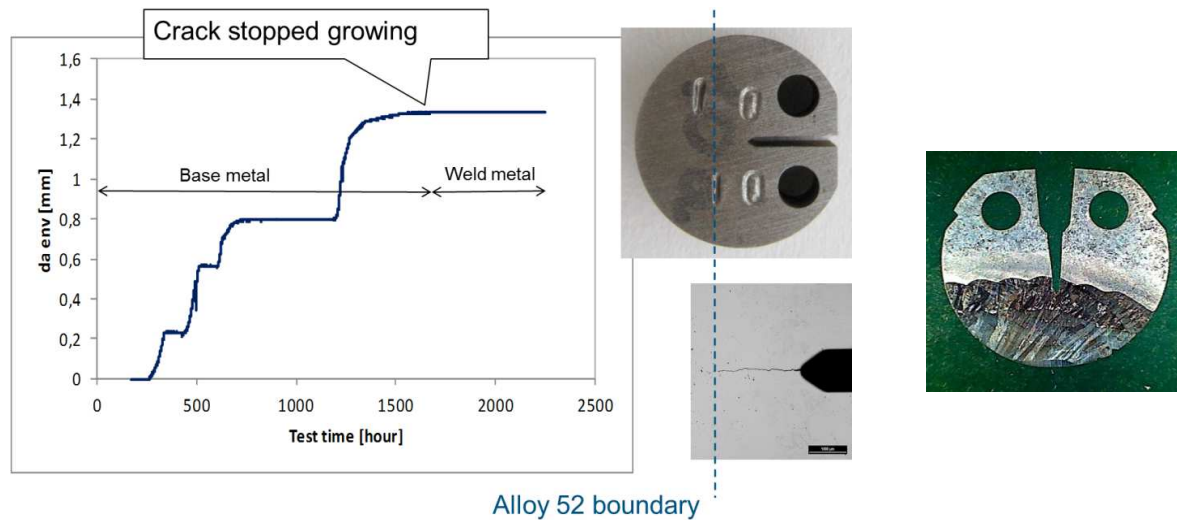


**Figure 25: Crack growth rate test with a DCT specimen of Alloy 52**

Four-point bending tests with Alloy 52 plates under PWR conditions were carried for 12 months. None of the four-point bending plates failed after 12 months of testing. If the non-failures are plotted on a time-to-failure plot, a result as shown in Figure 26 is obtained. An apparent threshold is then obtained of approximately 570MPa. Notice that this threshold can be higher, if testing were to be repeated with higher applied stresses, or lower when longer test times are used.

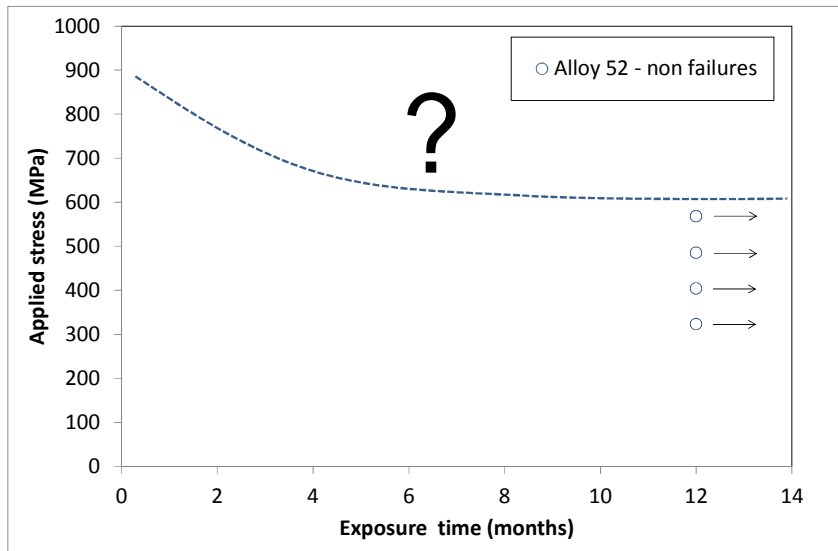


Figure 26: Time-to-failure plot showing an apparent stress threshold of 570 MPa

Achievements, lessons learned, and progress against STYLE objectives:

The SSRT tests showed that Alloy 52 has a high resistance to SCC in PWR primary water: there was no difference in strain to-failure between the test in PWR water and argon (= inert environment). The crack growth rate tests showed similar behaviour. There was no measurable crack growth in Alloy 52. An upper limit for CGR could be set, based on the resolution of the test equipment and test time. A typical upper bound crack growth rate of  $\leq 10^{-9}$  mm/s ( $\approx \leq 0.03$ mm/year) was obtained.

The crack initiation or time-to-failure test should determine a stress threshold below which no stress corrosion cracking will occur. With the four-point bending test eight specimens were tested, but none of them failed after 12 months testing. Therefore a critical stress limit has been set  $\geq 570$  MPa.

Experimental results obtained here show that Alloy 52 has a high resistance to stress corrosion cracking. This means that the experimental data are difficult to use in an empirical model. Therefore the modelling work is focussed on Alloy 182, for which a lot of data is available and empirical laws for crack growth (like MRP-115) and crack initiation (WinPRAISE07 and xLPR) are available. The models for Alloy 182 can then be transferred to Alloy 52 models with so called "improvement factors". With these "improvement factors" an engineering curve like a crack growth rate law can be defined. For the crack growth rate of Alloy 52 an improvement factor can have a value of 300 to 800 lower than the crack growth rate of Alloy 182 under similar conditions.

### 1.3.6 Thermal fatigue through turbulent mixing

Turbulent mixing of hot and cold water may lead to high-cycle thermal fatigue in nuclear power plant components. The fatigue phenomenon involves relatively high-frequency fluid temperature fluctuations near a solid wall, resulting in cyclic stresses in the wall material. This fatigue phenomenon is rather complex and of multidisciplinary nature, and no generally and fully accepted assessment procedure yet exists. One of the main difficulties in the modelling is determining the thermal load experienced by the structure.

A simplified method for predicting the phenomenon is the sinusoidal (SIN) method, where the thermal load is reduced into a sinusoidal time-variation having frequency which results in the shortest lifetime. Temperature range is usually chosen as the difference between the hot and cold fluid (or 80% of this) and the Heat Transfer Coefficient (HTC) may be e.g. scaled up conservatively from engineering correlations of fully developed pipe flow. The thermal stresses and the fatigue lifetime are then calculated with a 1D model representing the wall material. The SIN method is easy

to use but its validity in different situations is still unclear and it has been proposed overly-conservative in some cases.

The phenomenon may also be modelled by using Computational Fluid Dynamics (CFD) with a Large-Eddy Simulation (LES) turbulence model. The CFD calculations may be coupled with a 3D FEM model of the structure to determine the fatigue damage. In addition to being already a practical analysis tool for certain cases, this approach can also yield valuable information for the validation and development of simplified methods.

High-cycle thermal fatigue in a mixing Tee was studied by calculations with the SIN and CFD-FEM methods. The aims were to study the phenomenon and the realistic HTC with detailed numerical simulations as well as to assess the validity of the SIN method by using different boundary conditions and input parameters.

The thermal mixing experiment performed by Vattenfall Research and Development separately from the STYLE project in 2006 was considered. The test facility shown in Figure 27 consists of a horizontal cold water pipe with inner diameter of 140 mm and a vertical hot water pipe with inner diameter of 100 mm. A constant flow ratio  $Q_{cold}/Q_{hot} = 2$  was used which resulted in approximately equal flow velocities in the cold and hot pipes. The cold and hot temperatures were 15°C and 30°C. The tests were carried out with Reynolds numbers in the inlet pipes of approximately  $0.5 \times 10^5$ ,  $1 \times 10^5$  and  $2 \times 10^5$ . Velocity profiles were measured with Laser Doppler Velocimetry (LDV) about 3 diameters upstream as well as about 2.6 and 6.6 diameters downstream of the T-junction. Temperatures were measured with thermocouples located about 1mm from the pipe wall.

For performing numerical thermal fatigue studies, the following procedure was used: i) the LESs were validated against the experiment by assuming adiabatic walls, ii) coupled CFD-FEM calculations were performed where the pipes were assumed to consist of stainless steel with wall thickness 9.6mm and iii) the temperature difference and hence also the thermal stresses were linearly scaled up to obtain significant fatigue. This resulted in fairly realistic turbulent mixing loads without the need to run many computationally expensive LESs. The properties of water and steel were taken at room temperature according to the experimental conditions.

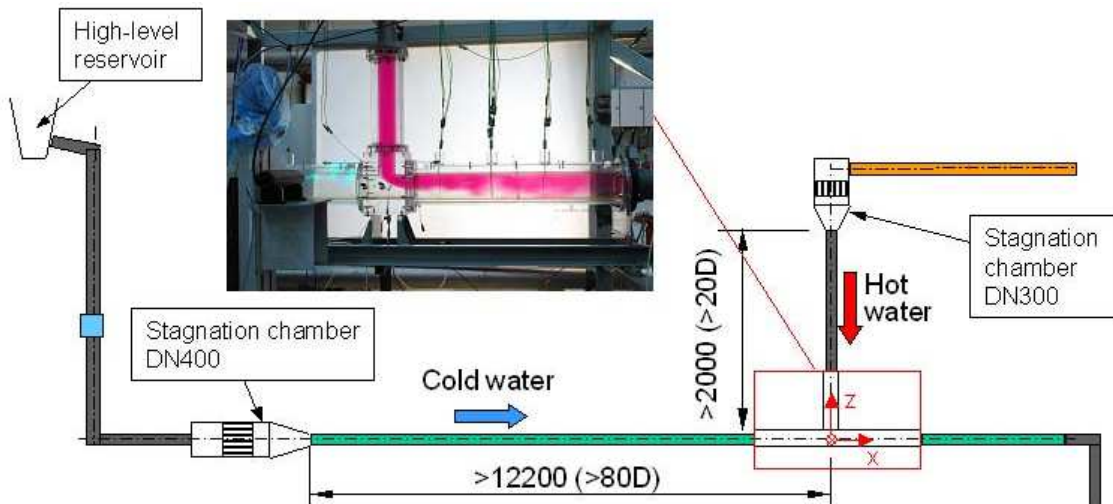


Figure 27: Vattenfall thermal mixing test facility

The conjugate heat transfer simulations were performed for three different flow rates as shown in Table 1. The cases with lower flow rates were obtained from Case 100% by linear scaling of both inlet flows. Note that only Case 50% and Case 100% were considered in the experiments.



**Table 1: Flow rates in the simulated cases. The Reynolds number and the viscous length scale are presented for the main pipe after the T-junction**

Case	Cold flow rate $Q_{cold}$ [l/s]	Hot flow rate $Q_{hot}$ [l/s]	Reynolds number	Viscous length scale [m]
15%	1.8	0.9	25569	$9.92 \times 10^{-5}$
50%	6	3	85231	$3.41 \times 10^{-5}$
100%	12	6	170461	$1.83 \times 10^{-5}$

The FEM analyses were performed by using the coupled temperature-displacement method of Abaqus, i.e. the transient temperatures and stresses in the structure were solved simultaneously. The backward Euler method was used for direct time-integration of the thermal field. Linear eight-node hexahedral elements with reduced integration were applied.

In the 3D models, the CFD meshes of the pipe wall were used as such. Fixed boundary conditions were applied only at the cold inlet end to prevent rigid body motion. No pressure load was applied, since the effects of static loads vanish in the fatigue calculation due to linearity of the model. The time step was the same as used in the load transfer.

The 1D model represented a sector of material column through the main pipe wall. Two different boundary conditions were used in the 1D model:

- BC 1: the tangential direction is fixed, while the axial planes are free to expand but forced to remain planar and oriented perpendicular to the pipe axis. This corresponds to the axisymmetric case of a long pipe with free ends.
- BC 2: the tangential and axial directions are both fixed. This corresponds to the axisymmetric case of a pipe with both ends fixed in the axial direction.

BC 2 gives higher stresses than BC 1 for low frequencies, while for high frequencies the results become practically identical.

RMS temperatures are shown at the steel pipe inner surface in Figure 28. The results for the different cases appear quite similar. The highest temperature fluctuations are found at the corner and right after the T-junction. When the flow velocity is lower, higher wall fluctuations are obtained near the corner. On the other hand, with a higher flow velocity the wall fluctuation intensity spreads longer along the main pipe. Interestingly, even for Case 100% the distributions with the coarse and fine meshes are quite similar, although for this flow case the near-wall density of the coarse mesh may be considered insufficient.

From the fatigue lifetimes calculated with different models the following main conclusions can be drawn from the results:

- Locations closest to the T-junction experience highest fatigue, as expected from the distributions of RMS temperature at the pipe inner surface.
- The lifetimes get generally shorter with increasing flow velocity due to increased HTC and frequency content of the fluctuations.
- The fine mesh yields shorter lifetimes than the coarse one. The differences are largest at the sharp corner. The trends are generally similar for both meshes.
- The 1D model yields shorter lifetimes than the 3D model for the corresponding temperature load. Differences between the 1D and 3D models are quite large at the sharp corner, since the 1D model describes a straight pipe section. For the straight pipe sections, the 1D model is fairly realistic.

- BC 1 is more realistic than BC 2 in this particular case, as it reduces the conservatism of the 1D model.
- Compared to CFD-FEM, the SIN method yields partly non-conservative results for the lowest flow velocity while overly conservative results for the highest flow velocity. Reasons for these differences are discussed below.

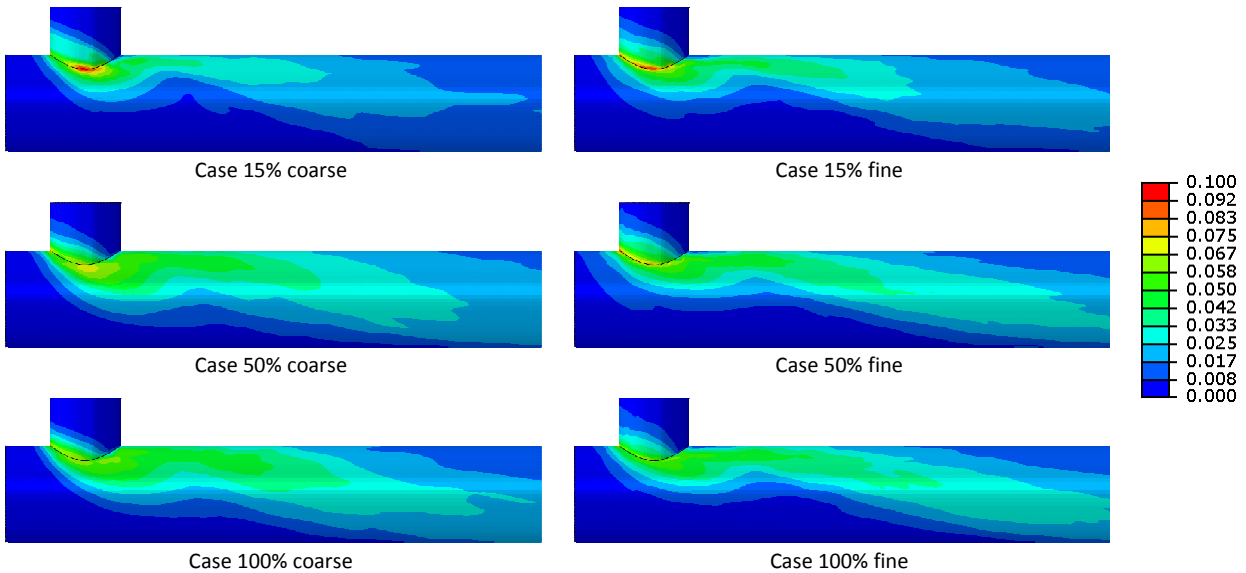


**Figure 28: Normalized RMS temperature fields at the steel pipe inner surface**

Achievements, lessons learned, and progress against STYLE objectives:

The mean and fluctuating components of velocity and temperature were in good agreement with the experiment when using the fine mesh. This shows the suitability of LES for modelling the turbulent mixing phenomenon. With the coarse mesh, in general qualitative agreement with the experiment was found. The adiabatic and coupled wall boundary conditions showed practically no differences in the logarithmic layer and upwards, whereas at the wall surface the difference becomes significant. Wall-resolved LES should be used in the CFD-FEM calculations rather than LES with wall functions, but the computational cost may still become prohibitively large for many real-life cases.

The highest wall temperature fluctuations and fatigue occurred near the T-junction. With a lower flow velocity, somewhat higher wall temperature fluctuations were obtained near the T-junction, whereas with a higher flow velocity the wall temperature fluctuations spread longer along the main pipe. The lifetimes got generally shorter with increasing flow velocity, which can be attributed to the increase of both HTC and frequency content. The coarse mesh resulted in notably longer lifetimes than the fine mesh, although the distributions of wall surface RMS temperatures were quite similar. Thus, the near-wall CFD-FEM mesh needs to be fine for accurate fatigue prediction.

Comparison of 1D and 3D models having corresponding temperature loads showed that the 1D model yields conservative lifetimes. The 1D model was overly conservative at the corner of the T-junction, while for the other locations agreement between the 1D and 3D models was quite good.

In the SIN method, the HTC was assumed to be 3 times the Colburn correlation based on HTCs deduced from LES. This resulted in lifetimes ranging from being non-conservative to overly conservative, depending on flow velocity, when compared to CFD-FEM. Lifetimes obtained with the SIN method dropped more rapidly than in the CFD-FEM calculations when the flow velocity was

increased. Firstly, results of the SIN method were sensitive to the HTC, for which best-estimate value was used. Thus, accurate estimation of the HTC is of great importance. The scaling factor of 3 was determined close to the corner, but the fatigue results indicate that right at the corner a higher scaling factor should be used. Also, the Reynolds number dependency of the HTC was weaker in the CFD-FEM calculations than in the correlation. Secondly, as noted above, the wall surface temperature fluctuations near the T-junction decreased somewhat with increasing flow velocity. Thirdly, the mesh density near the pipe inner surface for both the fluid and solid domains in the CFD-FEM calculations may become insufficient for the higher flow velocities, thus showing possibly non-conservative lifetimes.

### 1.3.7 Dynamic and impact effects - Mock-up 7

Mock-up 7 (MU7) was designed to investigate effects that have to be considered in a dynamic loading condition, and their implications on a LBB assessment. Although a seismic event would result in a more general cyclic loading case, the test programme was addressed specifically at impact loads that may occur in a sudden singular movement of, for example, the end of a pipe, due to an impact. A key parameter is the crack tip loading rate,  $dK/dt$ , which can vary with the assumed loading condition and component geometry. For impact events,  $dK/dt$  is approximately  $10^5 \text{ MPa}\sqrt{\text{m}} \text{ s}^{-1}$  for an impactor speed of  $v_0 = 5\text{m/s}$ .

Fracture properties such as the fracture toughness values  $K_{Jc,d}(T)$ , and fracture-resistance curve  $J_{mat}-R(T)$  change with increasing loading rate. For ferritic steels such as the tested 16Mo3, dynamic toughness vs. temperature curves  $K_{Jc,d}(T)$  are shifted in the lower shelf and transition range towards higher temperatures by  $\Delta T(dK/dt)$ , which results in a decrease in fracture toughness due to the dynamic embrittlement. On the other hand, in the upper shelf range  $J_{mat}-R$  values increase with increasing loading rate. However, due to dynamic embrittlement and the shift of the fracture toughness curve  $K_{Jc,d}(T)$  even at these higher temperatures in the upper shelf region a change from ductile to brittle behaviour has to be considered. This can be seen schematically in Figure 29.

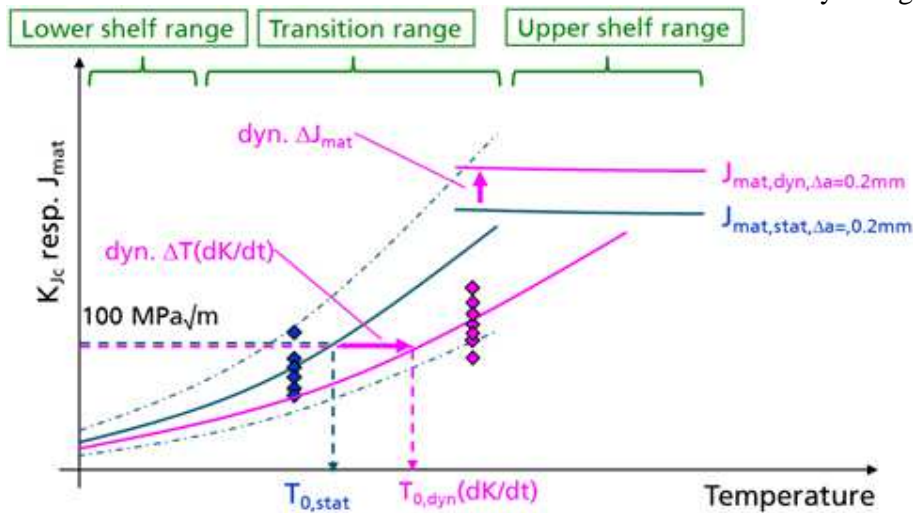


**Figure 29: Material behaviour, fracture toughness resp. fracture resistance vs. temperature, comparison of quasistatic and dynamic loading**

The MU7 test set-up consisted of a pipe that is rotationally fixed at one end. The dynamic load was applied at the other end with a drop weight tower. The mass of the impactor is 285 kg. The initial height was set to achieve a velocity  $v_0$  at impact of 5m/s for the first two tests and 6m/s for the third test, which results in a crack tip loading rate of around  $dK/dt \approx 10^5 \text{ MPa}\sqrt{\text{m}} \text{ s}^{-1}$  at the beginning of the tests. The test set-up including the fixation at one side of the pipe is shown schematically in Figure 30. The distance between applied load and crack measured  $l = 400\text{mm}$ .

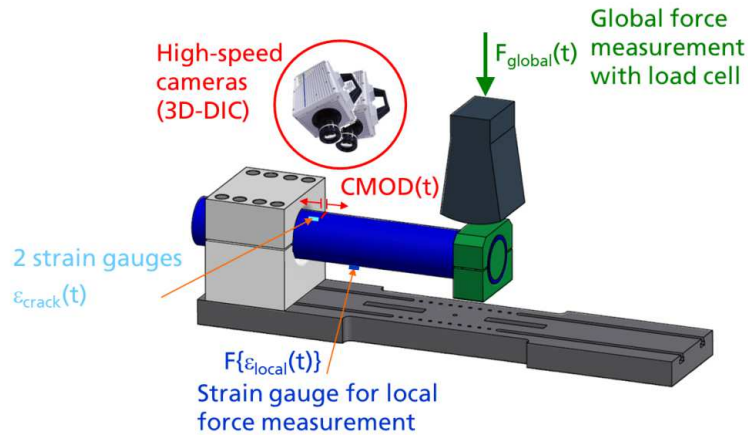


**Figure 30: Test set-up of Mock-up 7**

Figure 31 shows the test set-up of Mock-up 7 with applied strain gauges and high-speed cameras to measure CMOD. A copper plate was attached at the free end of the pipe in order to reduce the first impact impulse between the impactor and the pipe and thus to minimise the initial peak in the measured global force signal.

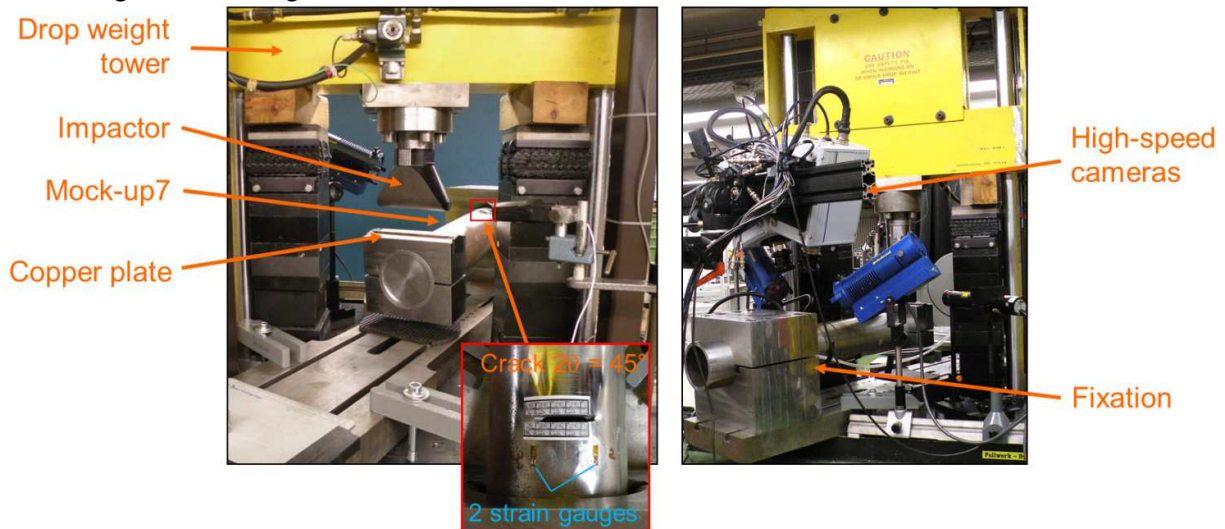


**Figure 31: Mock-up 7 after testing under the drop weight tower**

As can be seen in Figure 32, the measured global force  $F_{global}(t)$  from the first and second test with  $v_0 = 5\text{m/s}$  showed large oscillations. Also a brief lift-off between impactor and pipe can be seen in the diagram where the global force signal is zero for a short interval.

For the test at  $v_0 = 6\text{m/s}$  it was expected that the global force exceeds (at the first instance of impact) the 500kN limit of the load cell. Therefore in this test the load cell was detached and only the local force was measured.

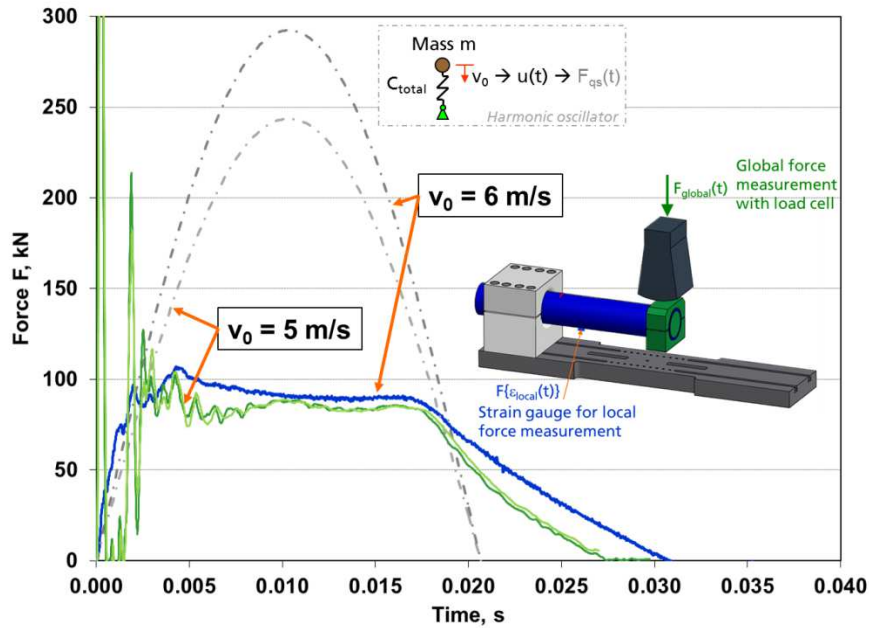


Figure 32: Global  $F_{\text{global}}(t)$  and local  $F\{\epsilon_{\text{local}}(t)\}$  force signal of the Mock-up 7 tests at two different loading velocities

The force over time can also be estimated by assuming that the dynamically loaded system of pipe, fixture and impactor act as an excited harmonic oscillator. Thus, only the mass and the compliance of the entire system  $C_{\text{total}}$  need to be known to calculate the global force for the elastic case, when no crack propagation and no plastic deformation take place. The result for one half period is plotted as dash-dotted grey lines in Figure 32 for the case of  $v_0 = 5 \text{ m/s}$  and shows a slightly higher curve for  $v_0 = 6 \text{ m/s}$ .

After the tests, the pipes were opened in the cold condition with liquid nitrogen and the fracture surfaces were investigated. The analysis with a scanning electron microscope (SEM) revealed a ductile crack surface. Figure 33 shows the SEM images zoomed to the transition from the fatigue pre-crack to the beginning of the ductile crack extension for a test with  $v_0 = 5 \text{ m/s}$ . The area of stable crack growth was measured afterwards with an optical measuring microscope.

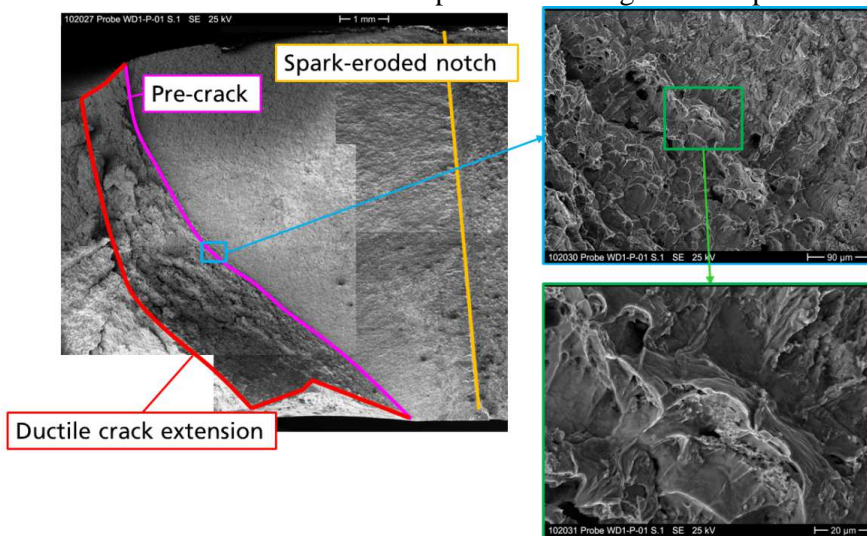


Figure 33: Transition from pre-crack to ductile crack extension (test at  $v_0 = 5 \text{ m/s}$ )

Achievements, lessons learned, and progress against STYLE objectives:

In summary the following conclusions can be drawn from the experiment and the evaluated numerical simulations.

Test set-up and measurements:

- Elastic wave propagation that leads to locally increased crack tip loading  $J(t)$  compared to the quasistatic  $J(t)$  curve played only a minor role for Mock-Up7, but could usefully be considered for other test arrangements e.g. with longer spans than the  $l = 450\text{mm}$  used here.
- A strain gauge attached on the opposite side of the crack was used for a local force measurement. The signal is not affected by the vibrational behaviour of the impactor and the load cell, and thus shows fewer oscillations and represents the actual crack tip loading more correctly.
- Near crack tip strain gauges showed clear deviation from the numerical results that assumed a stationary crack, thus indicating the time of crack initiation.
- CMOD(t) was captured with highspeed cameras, and was used along with the local force measurement  $F\{\varepsilon_{\text{local}}(T)\}$  in order to evaluate the crack tip loading  $J(t)$  experimentally.

Dynamic material behaviour:

- Embrittlement due to dynamic impact loading was investigated here. Contrary to the possible brittle fracture behaviour at room temperature, that was predicted by the extrapolated Master Curve approach with small SE(B) specimen tests at  $-20^{\circ}\text{C}$ , the actual MU-7 tests at room temperature showed ductile crack extension and crack arrest. This can be explained by the lower triaxiality (ie low constraint) at the crack front in the case of the pipe geometry ( $h \approx 1.6$ ) when compared to the tested small scale SE(B) specimens ( $h \approx 2.25$ ) with a different constraint condition. Thus, concerning the transferability of fracture properties: fracture toughness from standard tests need to be adjusted when compared to component tests due to different constraint conditions, but enable a conservative fracture assessment.
- A dynamic J-R curve was roughly 10% higher than the quasistatic one and should be used to predict crack initiation.
- The strain rate effect showed an increase of the true stress-strain curves by 20% ( $d\varepsilon/dt = 100 \text{ s}^{-1}$ ) and has been considered in the numerical simulations.

Numerical simulations:

- An assumed stationary crack in the FE simulations lead to higher  $J(t)$ -curves than the  $J(t)$ -curves obtained from the experimental data and the analytical formulas. Therefore, numerical simulations should also consider a propagating crack.

LBB assessment:

- LBB assessment of the pipe showed through wall penetration before the critical crack length was reached, i.e. leak before complete failure.

### 1.3.8 LBB approaches and Engineering Assessment Methods

#### Qualitative comparison of leak-before-break methodologies and licensing position:

A qualitative overview of leak-before-break (LBB) national practices and the regulatory position for the different participants was undertaken early in the STYLE project. The organisations which took part were AREVA-GmbH (Germany), CEA (France), AMEC (UK), AEKI (Hungary), UJV (Czech Republic), TEC (Spain), NRG (Netherlands) and ORNL (USA). (ORNL is linked to the STYLE

project on a “contribution in kind” basis.) Each participant was asked to compile an overview of LBB practices for their respective country under the following headings:

- Outline of LBB practice
- Outline of regulatory position
- Outline of evolution of LBB
- Application of LBB
- Past, present and planned future LBB research activities
- Future LBB plans.

The review indicated that the main distinction between different countries is in what procedure is adopted. The two main LBB procedures adopted are the LBB procedure as a part of the Break Preclusion Concept/Integrity Concept (BPC/IC) of Germany and SRP 3.6.3 of the USA. LBB procedures contained in the R6 and RCC-MRX procedures are also used, but only generally in the UK and France, respectively.

All LBB procedures adopt a similar approach in making the basic case for an LBB argument. The argument simply states that a crack should be large enough so that the loss of fluid escaping the through wall crack can be detected, whilst remaining small enough that structural failure of the pipe does not occur. Some further commonalities are that there is a minimum pipe diameter requirement and a restriction to high pressure piping. This generally limits the use of LBB to the main coolant lines, surge lines, accumulator lines, Emergency Core Cooling System, steam lines and feed-water lines (note the last two are excluded by SRP 3.6.3 if non quantifiable flow assisted corrosion (FAC) occurs).

The use of LBB in both the UK R6 and German BPC/IC approaches share many similarities in that they are adopted as defence in depth approaches. These approaches are therefore more general and allow greater freedom in applicable conditions and safety requirements, whereas the US SRP 3.6.3 approach places more stipulations on suitable piping, environmental and loading conditions.

Historically, all of the approaches were developed through the 1970s and 1980s with initial versions of the existing procedures in place between 1979 and 1990. A number of programmes, computer codes and experiments performed during this development have been identified.

Current and future plans on LBB research are limited and primarily confined to the critical crack size assessment and crack opening area (COA) determination. Two additional research areas are identified as application to Dissimilar Metal Welds (DMWs) and Weld Overlays (WOLs), as well as probabilistic assessments, potentially allowing LBB approaches to be negated.

It is also clear that, especially in countries where LBB is not currently adopted, future plans include the use of LBB for new-build power plants.

### **Qualitative overview of Engineering Assessment Methods:**

A qualitative comparison of Engineering Assessment Methods (EAMs) was undertaken by collating relevant information collected from the various participants. The organisations which took part were AREVA-GmbH (Germany), AREVA-F (France), CEA (France), AMEC (UK), University of Bristol (UK), NRG (Netherlands), UJV (Czech Republic), TEC (Spain), VTT (Finland) and Ringhals (Sweden). The main aspects of the study were related to Mock-Up Experiments 1, 2 and 3. The individual partners were thus asked to provide brief descriptions of their EAMs for structural integrity evaluations of dissimilar metal welds, repair welds and clad ferritic pipes. In their contributions, special attention was intended to be focussed on such aspects as mismatch of material properties, residual stresses, mixed-mode loading and constraint effects.

In studying the contributions received from the participants, several types of commonalities were evident. The first commonality relates to the use of a commonly adopted assessment code or methodology. Nearly all partners reported using the ASME Code (either as their main assessment code or in addition to their national codes). Use of the R6 methodology and the KTA standard outside the UK and Germany (respectively) was reported not to be very common and the French standards RCC-M, RCC-MRx or RSE-M are mainly specific to France. For assessing the three types of structural features considered though, many of the participants reported that they would undertake detailed finite element analyses, as a supplementary or as an alternative to their codes or procedures. Another common feature was identified as being that practically all of the assessment methods and codes (ASME Code, R6, VERLIFE, KTA and others) specified the use of conservative material properties, at least in the first instance. A further commonality relates to the fact that in assessing flaws in clad ferritic piping, the actual cladding is generally not taken into account which is considered to be conservative.

Several differences between the various EAMs were identified. One difference is the definition of flow stress relating to limit load analysis. Flow stress is defined as the average of the yield stress and ultimate tensile stress in R6 and Appendix C of ASME III. In the German approach, flow stress is derived from data obtained from a large number of small-scale and structural specimens. Another difference between the individual EAMs is associated with the provision of guidance for treating weld residual stresses when assessing flawed component. Whilst, for example, the R6 methodology provides detailed guidance on how to determine the residual stress variation in the weld, some other codes, such as the French, provide practically no guidance. Traditionally, only R6 allows for strength mismatch to be taken in to account but this aspect has also recently been incorporated into the French codes. Finally, R6 is the only methodology which, as one of its higher level methods, contains a procedure for allowing for crack-tip constraint effects.

### **Qualitative overview of probabilistic methods:**

A qualitative overview of state-of-art probabilistic approaches to Engineering Assessment Methods, including Leak Before Break, in various countries was undertaken. Whilst it was intended for the overview to be relevant to all European countries, it primarily focuses on France, Germany, UK, Spain, Hungary, the Netherlands, Romania and the Czech Republic. The overview includes LBB applied to PWR, BWR, VVER, PHWR and AGR types of reactors. The overview includes such aspects as specific failure events and methods of analysis for piping, uncertainties of input parameters (e.g. loading conditions, material properties, flaw size, flaw detect ability) using different methods (Monte-Carlo, FORM, SORM). The position of the USA is represented by ORNL, which is running a parallel project with similar objectives to STYLE (as previously stated, ORNL is linked to the STYLE project on a “contribution in kind” basis).

Each participant was asked to compile an overview of LBB practices for their respective country under specific headings. Based on the input received from the STYLE partners, it could be concluded that there are two great poles of systematic studies on probabilistic approach in the EAM (LBB) domain, namely in the UK and the US. Both approaches are based on the probabilistic fracture mechanics principle, and use similar steps as in deterministic assessment methodology. Probabilistic approaches of EAM (LBB) of other countries in this area revolve more or less around either of these two approaches.

Despite the fact that probabilistic fracture mechanics techniques have been developed over a number of years in the UK, Germany, the US and other countries as a possible means of quantifying the integrity of structures, probabilistic approaches of EAM and LBB are still under development. In principle, the regulatory position is generally to consider the probabilistic EAM for sensitivity studies and estimation of margins as additional analyses to the conservative deterministic analyses.



Computer codes have been developed and used for inter-comparative analyses (STAR 6, PROF, PRAISE, and PROSINTAP). Recently, in the UK a new software code, PFMAD (Probabilistic Fracture Mechanics and Design), based on probabilistic fracture mechanics using the R6 procedure, has been developed by AMEC (for R&D studies only at this stage). Also, in the US a multi-year xLPR (eXtremely Low Probability of Rupture) Project is underway with a focus on developing a viable method and approach to address the effects of PWSCC and on defining the requirements for a modular-based assessment tool.

Achievements, lessons learned, and progress against STYLE objectives:

- For LBB assessments, the main distinction between different countries is in what procedure is adopted. The two main LBB procedures adopted are the LBB procedure as a part of the Break Preclusion Concept/Integrity Concept (BPC/IC) of Germany and SRP 3.6.3 of the USA. LBB procedures contained in the R6 and RCC-MRX procedures are also used, but only generally in the UK and France, respectively. Whilst there are several commonalities and differences in the detail, all the procedures adopt a similar approach in making the basic case for an LBB argument. The argument simply states that a crack should be large enough so that the loss of fluid escaping the through wall crack can be detected, whilst remaining small enough that structural failure of the pipe does not occur.
- For EAM assessments in general relating to structural integrity evaluations of dissimilar metal welds, repair welds and clad ferritic pipes, several commonalities and differences are evident. The commonalities include the use of a commonly adopted assessment code or methodology, usually supplemented by detailed finite element analyses, the use of conservative material properties and in the case of clad pipes, excluding the actual cladding in the evaluations which is considered to be conservative. The differences include the definition of flow stress, the provision of guidance for treating weld residual stresses and the incorporation of higher level methodology such as weld strength mis-match and crack-tip constraint effects.
- Deterministic EAMs for evaluating fracture conditions in complex geometries like dissimilar metal welds, repair welds and clad ferritic pipes can provide a variety of results depending on the method and the selection of input data used. The EAM results have generally been shown to be conservative with respect to the Mock-Up experimental results, particularly for evaluating such aspects as Crack Opening Displacement and applied load for initiation of tearing. Not surprisingly, the input data which can have a significant influence on the EAM results are the tensile and fracture properties used and various assumptions on weld residual stresses.
- Probabilistic evaluations applied to a case study based on the Mock-Up 2 experiment have indicated that the calculated probabilities of tearing initiation are in good agreement between the various participants. Overall, the probability predictions for net-section collapse have been found to be in reasonable agreement with respect to a variety of different methods used. Sensitivity studies have indicated that the variability in crack size is more sensitive than the variability in residual stress in relation to tearing initiation evaluation.

Recommendations:

- Where possible, sensitivity studies should be included in EAM (and LBB) evaluations in order to assess the significance on the results of varying the input data, particularly for defects located in a region of composite material and/or of significant residual stress.
- Additional EAM, finite element analyses and analysis of the Mock-Up experimental data needs to be undertaken in order to pave the way for developing general unified guidance for

undertaking fracture assessments in complex geometries like dissimilar metal welds, repair welds and clad ferritic pipes.

- In association with the developed guidance, work is required in order to be able to recommend conservative (but not too conservative) weld residual stress profiles for the structural features under consideration.

### **1.3.9 Training**

Training has been based on the experimental and analytical work carried out under other STYLE project work packages and has generally taken the form of dedicated visits, typically a few days in duration, to the relevant host organisations' establishment. The various training topics include experimental work, numerical modelling and simulation (residual stress, welding, environmentally assisted cracking and the effects of dynamic/seismic loading on components), engineering assessment procedures, probabilistic fracture mechanics and materials behaviour.

Training course proposals were developed by the relevant hosting organisations and provided to the candidates. The content of these documents includes a description of the training task to be performed within the project, a list of relevant reference material including technical papers and relevant code and standards, together with detailed time schedule and reporting arrangements. A structured process was established to coordinate applications and selection of eligible persons. The STYLE project general assembly approved the nomination of training candidates, following consideration of the goals and expected results associated with each training visit.

An extensive suite of documents has been developed to specify and record training events. This includes training proposals and presentations produced by host organisations and also reports provided by attendees to record feedback following receipt of training.

A Training Handbook has been produced, based on material developed to support the training events. Seven training modules are included in this manual, based on case studies described in previous sections, the technical topics addressed in the manual being as follows:

- Module 1 Transferability
- Module 2 Dissimilar Metal Welds
- Module 3 Leak-Before-Break
- Module 4 Stress Corrosion Cracking
- Module 5 Seismic/dynamic effects
- Module 6 Thermal fatigue due to turbulent mixing
- Module 7 Residual Stress

It is intended that the manual will be used by organisations that have participated in the STYLE project to facilitate future modular training in key areas of structural integrity assessment of reactor coolant pressure boundary components relevant to ageing and lifetime management.

### **1.3.10 Main project conclusions (final summary)**

#### **1) On narrow gap dissimilar metal weld integrity**

##### Implications

- The stress-strain curves for all the materials have been tested in STYLE and the results highlight the gradient of properties in these multi-materials.

- From the fracture test and interpretation of multi-material CT specimens it could be seen that there is a large scatter in the fracture toughness values. A large effect of the distance from the interface Inconel/ferritic steel (FS) has been observed.
- The large scale test was a case study on a 4-point-bending test with a through crack at the weakest location (interface of Inconel/FS). The test has been performed at 300°C.

#### Recommendations

- A combination of micro-hardness test and of experimental and numerical methodologies to determine stress-strain curve for all materials is recommended.
- FE support is essential for the evaluation multi-material CT specimen results.
- An energy approach called J/Gfr can be used to predict crack growth in the large scale test for initiation and ductile tearing.

#### Open issues

- A further development of numerical tools to predict the complete fracture behavior of components (ductile tearing with deviation from the initial crack location) is necessary. EAM tools and advanced tools including local approach have to be considered for this purpose.

### **2) On effects of residual stress on ductile fracture and damage modelling**

#### Implications

- Localised repair welding introduces high membrane residual stresses that contribute to initiation of ductile tearing but are rapidly accommodated by plastic deformation.

#### Recommendations

- In ductile materials the presence of residual stress has no influence on global collapse but has a significant influence of local collapse (and ductile crack initiation). It is recommended that local collapse solutions should not be used in structural integrity analyses.

#### Open issues

- Ageing embrittlement lowers fracture energy for initiation and growth of defects. Ageing will also reduce repair weld residual stress, but these may still play an important role in long term ageing.

### **3) On transferability of material properties**

#### Implications

- J- $\Delta a$  curves from small scale specimens with deep cracks lead to conservative fracture mechanics assessment of large scale components
- Experiments on small scale specimens confirm the independency of crack initiation of crack tip constraint in the ductile regime. Cruciform and 3PB specimens show no biaxial loading effect on crack initiation and crack propagation in small scale specimens.
- The cladding affects considerably the components limit load, there is approx. 12% additional safety margin gain if the cladding is considered in the limit load analysis

#### Recommendations

- All standard fracture mechanics specimens can be used for conservative assessment of components in ductile regime.
- Ductile crack initiation can be treated as independent of crack geometry and loading
- Biaxial loading need not be considered on ductile crack initiation and growth

#### Open issues

- Further development of numerical tools to predict complete fracture of components (ductile to brittle transition - change of crack mechanism)

#### **4) On weld residual stress simulation and measurement**

##### Implications

- The simulation of the welding process needs much processing power and long time.
- The material data are quite often incomplete, specifically data at all relevant temperatures up to melting temperature.
- The numerical simulation can be numerically unstable, some solvers, although quicker are not as robust as others - an example is the multi-frontal sparse vs. the iterative sparse.

##### Recommendations

- Time, disk space and high processing power should be provided for a successful simulation of welding.
- The missing material data should be identified and measured if possible.

#### Open issues

- For the weld residual stress modelling of austenitic similar metal welds it is necessary to handle correctly large distortions in thin-walled pipes.
- The reliability of 3D analyses of repair-welded pipes is still quite improvable.
- The impact of load history (especially residual stress) on ductile damage models and actual behaviour is not fully understood.
- EAM such as R6 should be improved for weld repair assessment.

#### **5) On stress corrosion cracking**

##### Implications

- Ni-based weld metal alloy 52 has a high resistance to SCC in PWR primary water
- There was no measurable crack growth in Alloy 52

##### Recommendations

- Upper limits for crack growth rate and SCC stress threshold were defined based on resolution of test equipment and test time. For the future tests it is recommended to set the test stress limit higher than 570 MPa.

#### Open issues

- In future projects longer test times and/or a reliable accelerated test method need to be used when testing SCC resistant materials

#### **6) On thermal fatigue through turbulent mixing**

##### Implications

- LES CFD is suitable for turbulent mixing modelling, but computational cost may still become prohibitively large for many plant cases.
- For coupled CFD-FEM, near-wall mesh needs to be fine for accurate fatigue prediction.
- 1D model gives fairly realistic and slightly conservative fatigue for straight pipe sections with realistic load, at corners more errors expected.
- SIN method results ranged from slightly non-conservative to overly conservative, depending on flow velocity, compared to CFD-FEM.

### Recommendations

- Wall-resolved LES should be used whenever possible in coupled CFD-FEM.
- Heat transfer coefficient should be estimated accurately for SIN method.
- Free pipe ends should be used rather than axially fixed pipe ends in SIN method.

### Open issues

- The heat transfer coefficient was shown to be a very important parameter for the simplified assessment methods and thus accurate determination of this parameter should be pursued. It should be studied whether the Reynolds number dependency of the maximum heat transfer coefficient is the same as in the correlations for fully developed flows
- For the coupled CFD-FEM calculations, the effect of mesh density near the walls should be studied further for both the CFD and structural models.

## **7) On dynamic and impact effects**

### Implications

- Assumed quasistatic instead of dynamic loads generally lead to conservative fracture assessments.
- J- $\Delta a$  curves from standard fracture mechanics specimens lead to conservative assessment of large scale components.
- Numerical simulations with stationary cracks overestimate crack tip loading after crack initiation.

### Recommendations

- Possible change from ductile to brittle fracture behaviour due to impact loading should be considered.
- FE simulations should include strain rate dependent material data.
- Depending on the geometry the effect of elastic wave propagation on crack tip loading might need to be considered in a dynamic FE analysis.

### Open issues

- Prediction of the dynamic Mastercurve considering the change from ductile to brittle fracture.

## **8) On LBB approaches and Engineering Assessment Methods**

### Implications

- EAMs for evaluating fracture conditions in complex geometries, like DMWs, clad pipes and repair welds, can provide a variety of results depending on the method and the selection of input data used.
- The EAM results have generally been shown to be conservative with respect to the Mock-Up experimental results, particularly for evaluating such aspects as COD and applied load for initiation of tearing.
- Not surprisingly, the input data which can have a significant influence on the EAM results are the tensile and fracture properties used and various assumptions on weld residual stresses.

### Recommendations

- Where possible, sensitivity studies should be included in EAM (and LBB) evaluations in order to assess the significance on the results of varying the input data, particularly for defects located in a region of composite material and/or of significant residual stress.

### Open issues

- Additional EAM, finite element analyses and analysis of the Mock-Up experimental data needs to be undertaken in order to pave the way for developing general unified guidance for undertaking fracture assessments in complex geometries like dissimilar metal welds, repair welds and clad ferritic pipes.
- General unified guidance needs to be developed for undertaking fracture assessments in complex geometries, like DMWs, clad pipes and repair welds.
- In association with the developed guidance, work is required in order to be able to recommend conservative (but not too conservative) weld residual stress profiles for the structural features under consideration.

## **9) On training**

### Implications

- The training programme has demonstrated how complex research projects may contribute to career development and maintaining a skills base in the nuclear industry.
- Wide range of technical training topics has been delivered.

### Recommendations

- The STYLE training manual provides a useful resource available to participant organisations for training in future.

### Open issues

- None.

## **1.4 POTENTIAL IMPACT, EXPLOITATION OF RESULTS AND MAIN DISSEMINATION ACTIVITIES**

The project has contributed to safe operation of existing nuclear power plants and to maintaining high safety standards due to more accurate assessment methods resulting in increased margin of safety. STYLE has reinforced the competitiveness of the European nuclear industry by the achievement of innovative research results in the field of maintenance of nuclear power plants and by the participation of leading industrial companies in this field. The project may have outstanding impact on national and international research activities concerning the use of advanced tools for structural integrity assessments, fracture mechanic testing and corrosion experiments. The project has been actively involved in specific European networks (e.g. NUGENIA), which are fed by national and international research activities. Within the planned training activities all partners (especially universities and research organizations) have been encouraged to promote studentship as well as to publish the results of their work in the open literature. An important part of the project has been to give students and young researchers the opportunity to work on challenging problems side by side with their more experienced colleagues. Taking all this into account the project has generated a remarkable added-value in maintaining and improvement of collaborative research activities in the field of nuclear energy in the European Union.

### Main dissemination activities:

The dissemination of project result has been conducted through different channels:

- Publications in intentionally recognized conferences,
- Organisation of dedicated workshops and
- Presentation and discussion of results in specific European networks.

### A list of selected publications:

<i>Title</i>	<i>WP No</i>	<i>Date</i>	<i>Conference</i>	<i>Venue</i>
<i>STYLE: Mock-up3 design - FE Simulation of crack growth in a clad ferritic pipe</i>	<i>1, 2</i>	<i>July 2010</i>	<i>PVP 2010</i>	<i>Seattle</i>
<i>STYLE: Project overview</i>	<i>All</i>	<i>July 2010</i>	<i>PVP 2010</i>	<i>Seattle</i>
<i>STYLE: Study on transferability of fracture material properties from small scale specimens to a real component</i>	<i>1, 2</i>	<i>July 2011</i>	<i>PVP 2011</i>	<i>Baltimore</i>
<i>ORNL Pre-Test Analyses of a Large-Scale Experiment in STYLE</i>	<i>1, 2</i>	<i>July 2011</i>	<i>PVP 2011</i>	<i>Baltimore</i>
<i>Csonkmakett: Gyártás, mérés, szimuláció (Nozzle MU: Manufacturing, measurements, simulations) - in Hungarian</i>	<i>1,2</i>	<i>April 2012</i>	<i>XXI. Nemzetközi Gépészeti Találkozó (XXI. International Conference on Mechanical Engineering) OGÉT</i>	<i>Arad, Romania</i>
<i>STYLE – A European project on structural integrity: Progress of the work after 2 Years</i>	<i>All</i>	<i>May 2012</i>	<i>3rd International Conference on NPP Life Management (PLIM) for Long Term Operations (LTO)</i>	<i>Salt Lake City</i>
<i>STYLE project: Large scale experiment on a clad ferritic pipe</i>	<i>1</i>	<i>July 2012</i>	<i>PVP 2012</i>	<i>Toronto</i>
<i>STYLE: Transferability of fracture materials properties updated experimental and analytical results</i>	<i>2</i>	<i>July 2012</i>	<i>PVP 2012</i>	<i>Toronto</i>
<i>The influence of long-range residual stress on plastic collapse and local yielding of internally pressurised pipes</i>	<i>2</i>	<i>July 2012</i>	<i>PVP 2012</i>	<i>Toronto</i>
<i>Effect of ageing on residual stresses in welded stainless steel cylinders</i>	<i>1</i>	<i>July 2012</i>	<i>PVP 2012</i>	<i>Toronto</i>
<i>The Importance of a Strong Training Element Within the European STYLE Project</i>	<i>5</i>	<i>July 2012</i>	<i>PVP 2012</i>	<i>Toronto</i>

<i>Analysis of Ductile Crack Growth in Pipe Test in STYLE Project</i>	2	July 2012	PVP 2012	Toronto
<i>STYLE: Comparison of Engineering Assessment Methods</i>	3	July 2012	PVP 2012	Toronto
<i>STYLE: Comparison of Leak-Before-Break Methodologies Applied in Europe</i>	3	July 2012	PVP 2012	Toronto
<i>Mechanical Characterization for a Large Test Design of a Dissimilar Metals Welding With a Narrow Gap Nickel Alloy Weld: Experimental and Numerical Analysis on Specimens</i>	1, 2	July 2012	PVP 2012	Toronto
<i>FE Residual Stress Analysis in a Narrow Gap Dissimilar Metal Weld</i>	2	July 2012	PVP 2012	Toronto
<i>Prediction and Measurement of Weld Residual Stresses in Thermally Aged Girth-Welded Austenitic Steel Pipes</i>	1, 2	July 2012	PVP 2012	Toronto
<i>The Delivery Of Technical Training Within The European STYLE Project</i>	5	July 2013	PVP 2013	Paris
<i>European Project on Structural Integrity STYLE: Project Status</i>	All	July 2013	PVP 2013	Paris
<i>Manufacture, Residual Stress Measurement and Analysis of a VVER-440 Nozzle Mockup</i>	1,2	July 2013	PVP 2013	Paris
<i>Style Project: Preparation and Interpretation of a Four Points Bending Tests on a EPR Type DMW Pipe Containing a Circumferential Through-Wall Defect (Presentation Only)</i>	1,2	July 2013	PVP 2013	Paris
<i>NUGENIA-STYLE - Structural Integrity for Lifetime Management – Non-RPV Components</i>	All	August 2013	SMiRT-22	San Francisco

### **1.5 STYLE CONSORTIUM, WEB SITE AND CONTACT DETAILS**

The STYLE consortium has consisted of 20 organisations from eleven EU member states and one collaborating Non-EU country (USA) each with a high percentage of nuclear power in the total national electricity production. The consortium has represented universities, research and engineering institutes, manufacturers, operators and industrial companies playing a long-term and active role in the field of nuclear technology. The project partners have covered a well addressed field of specific expertise, staff and resources which is suited uniquely to the objectives of the proposed project. The consortium has been well balanced due to the participation of almost all EU countries involved in the research field nuclear energy.

The web site of the project has been designed as a friendly user platform that will allow a better coordination of the activities, and a smooth communication between the partners. It offers public information such as a project overview, the publishable information from the project reports, the list of project participants, etc. There is also a confidential part of the website accessible to



STYLE partners only. This area contains the STYLE document repository and a work area where documents under development can be exchanged amongst the partners. Other features in the confidential area include a STYLE internal calendar, and a discussion board.

The website address is: <http://style.jrc.ec.europa.eu/>

Contact details: Elisabeth Keim, the project coordinator  
[elisabeth.keim@areva.com](mailto:elisabeth.keim@areva.com)  
+49 9131 900 95218  
AREVA GmbH  
Postfach 1109  
91001 Erlangen  
Germany